Universidade Federal do Rio Grande – FURG

Instituto de Oceanografia

Programa de Pós-Graduação em Oceanologia

DINÂMICA DE MASSAS DE ÁGUA, MACRONUTRIENTES INORGÂNICOS E CLOROFILA NA REGIÃO DA CADEIA VITÓRIA-TRINDADE, OCEANO ATLÂNTICO SUDOESTE

ELIS BRANDÃO ROCHA

Dissertação apresentada à coordenação do PPGO como requisito parcial para a obtenção do título de mestre.

Orientador: *Prof. Dr.* CARLOS FRANCISCO FERREIRA DE ANDRADE

Coorientadora: *Profª. Drª.* EUNICE DA COSTA MACHADO

Universidade Federal do Rio Grande (FURG), Brasil

Rio Grande, RS, Brasil

Junho, 2019.

DINÂMICA DE MASSAS DE ÁGUA, MACRONUTRIENTES INORGÂNICOS E CLOROFILA NA REGIÃO DA CADEIA VITÓRIA-TRINDADE, OCEANO ATLÂNTICO SUDOESTE

Dissertação apresentada ao Programa de Pós-Graduação em Oceanologia, como parte dos requisitos para a obtenção do Título de Mestre.

por

ELIS BRANDÃO ROCHA

Rio Grande, RS, Brasil

Junho, 2019.

ROCHA, ELIS BRANDÃO

Dinâmica de massas de água, macronutrientes inorgânicos e clorofila na região da cadeia Vitória-Trindade, Oceano Atlântico Sudoeste / Elis Brandão Rocha. – Rio Grande: FURG, 2019.

Número de páginas 78 p.

Dissertação (Mestrado) – Universidade Federal do Rio Grande. Mestrado em Oceanologia. Área de Concentração: Oceanografia Química.

1. Macronutrientes Inorgânicos. 2. Massas de Água. 3. Clorofila. 4. Efeito Monte Submarino. 5. Cadeia Vitória-Trindade. 6. Oceano Atlântico Sudoeste. Dinâmica de massas de água, macronutrientes inorgânicos e clorofila na região da cadeia Vitória-Trindade, Oceano Atlântico Sudoeste.

ATA DE DEFESA

Agradecimentos

Aos meus pais, Angela e Luis, assim como toda minha família, por todo amor, investimento, incentivo e apoio. Amo e admiro vocês.

Aos meus orientadores, Carlos e Eunice, pela dedicação e comprometimento. Obrigada por serem sempre disponíveis para ajudar, aprendi muito com vocês.

Aos integrantes da banca examinadora, Mariele, Rodrigo e Kátia, obrigada pelas contribuições.

A todos os amigos da Hidroquímica, obrigada pela convivência, amizade, ajuda, conselhos e companheirismo.

A todas as pessoas que auxiliaram na elaboração deste trabalho, especialmente ao Fujita, o Lucas, a Raynara, o Gabriel e a Any.

Ao Rapha, que, literalmente, ajudou em todas as etapas desse trabalho. Muito obrigada pela parceria, em todos os momentos <3.

À Katarina, minha companheirinha inseparável.

A todos os meus amigos, obrigada por fazerem meus dias mais leves e felizes.

A todo corpo docente do PPGO por todo conhecimento passado.

À FURG, por ser essa universidade maravilhosa, na qual me sinto em casa.

Ao CNPq pela bolsa de estudos.

E por fim, a todos que, direta ou indiretamente, contribuíram para elaboração deste trabalho.

Índice

Lista de Figuras da Dissertação

Lista de Figuras do Manuscrito

Lista de Tabelas

Lista de Acrônimos e Abreviações

AABW: Antarctic Bottom Water

AAIW: Antarctic Intermediate Water

AOU: Apparent Oxygen Utilization

BC: Brazil Current

CRM: Certified Reference Material

DL: Detection Limit

DWBC: Deep Western Boundary Current

eOMP: Extended Optimum Multiparameter Analysis

ICW: Indian Central Water

IWBC: Intermediate Western Boundary Current

MLD: Mixed Layer Depth

N: Nitrate

NADW: North Atlantic Deep Water

NBC: North Brazil Current

O: Dissolved Oxygen

P: Phosphate

QL: Quantification Limit

R_x: Remineralisation ratio of ‘x’ inorganic macronutrient

S: Salinity

SACW: South Atlantic Central Water

SAO: South Atlantic Ocean

SEC: South Equatorial Current

Si: Silicate

SWT: Source Water Type

T: Potential Temperature

TW: Tropical Water

UCDW: Upper Circumpolar Deep Water

VTC: Vitória-Trindade Chain

[x]/[P]: Concentration ratio of ‘x’ inorganic macronutrient in relation to P

WOCE: World Ocean Circulation Experiment

WSDW: Weddell Sea Deep Water

Resumo

Neste trabalho, apresenta-se a distribuição dos macronutrientes inorgânicos (nitrato, fosfato e silicato) e das propriedades hidrográficas ao longo de duas seções no oeste do oceano Atlântico Sul, localizadas na Cadeia Vitória-Trindade e amostradas durante o verão austral de 2017. A presença de feições topográficas em oceanos oligotróficos é recorrentemente associada a maiores taxas de produção primária, assim como permite maior abundância microbiológica e biomassa de consumidores, devido ao maior fluxo de nutrientes para a zona eufótica. Entretanto, não foram encontradas maiores concentrações de macronutrientes inorgânicos próximo à superfície dos montes submarinos, consequência de uma forte estratificação da coluna de água observada para o verão. Ainda assim, foi observado um máximo de clorofila subsuperficial, apresentando concentrações duas vezes maiores nos cumes dos montes submarinos. Fazendo uso de tais propriedades hidrográficas e químicas, foram analisadas as distribuições e contribuições das águas-tipo fonte presentes ao longo das duas seções amostradas através da ferramenta *extended Optimum Multiparameter Analysis.* A distribuição das massas d'água na área de estudo mostrou-se amplamente consistente com resultados anteriores para o oeste do oceano Atlântico Sul subequatorial, exibindo, no entanto, a presença de um núcleo de Água Intermediária Antártica mais recentemente ventilada no canal mais *inshore*, entre o monte Vitória e a plataforma continental.

Palavras-chave*:* Macronutrientes Inorgânicos; Massas de Água; Clorofila; Efeito Monte Submarino; Cadeia Vitória-Trindade; Oceano Atlântico Sudoeste.

Abstract

We present the distribution of inorganic macronutrients (nitrate, phosphate and silicate) and hydrographic properties along two sections in the western South Atlantic Ocean, located in the Vitória-Trindade Chain region. The survey was conducted during austral summer of 2017. The presence of topographic features in the oligotrophic ocean is often related to the higher primary production rates, which in turn sustains higher microbial abundance and consumers biomass, due to the higher flux of nutrients to the euphotic zone. Despite that, it was not observed higher inorganic macronutrient concentrations in the surface at the seamounts, as a result of the strong summer shallow stratification. Furthermore, it was observed a deep chlorophyll maximum that presented 2-fold higher concentrations at the seamounts' summits. Using these hydrographic and chemical proprieties, we performed an extended Optimum Multiparameter analysis to diagnose the relative contributions of various water types along the sections and rationalize their distributions. The water mass compositions appear largely consistent with what is understood from previous studies for the subequatorial western South Atlantic. However, it was found higher concentration and more recently ventilated Antarctic Intermediate Water in the inshoremost channel between the Vitória seamount and the continental shelf.

Keywords*:* Inorganic Macronutrients; Water masses; Chlorophyll; Seamount Effect; Vitória-Trindade Chain; Southwestern Atlantic Ocean.

Capítulo I:

Introdução

1. Introdução

A produção primária nos oceanos é fundamentalmente realizada pelo fitoplâncton, que converte dióxido de carbono e macronutrientes inorgânicos (como o nitrato, o fosfato e o silício) em matéria orgânica, através da fotossíntese (Lalli & Parsons, 1997). Sendo assim, a produção de energia nos sistemas oceânicos é dependente das concentrações de macronutrientes, dióxido de carbono, temperatura e da disponibilidade de luz no ambiente.

As concentrações de macronutrientes nos oceanos são controladas por vários processos de aportes e perdas. A chuva e os rios lixiviam as rochas continentais, carregando seus constituintes para as regiões costeiras, enquanto o vento carrega partículas em suspensão da atmosfera para as regiões oceânicas (Castello & Krug, 2015). Dessa forma, as plataformas continentais costumam ser mais enriquecidas em macronutrientes em comparação ao oceano aberto, devido a maior proximidade com o continente.

Nas regiões oceânicas, as principais fontes de macronutrientes são resultado de fluxos verticais (advecção e difusão) de águas mais profundas e ricas para as camadas superficiais (eufóticas) dos oceanos, além da remineralização da matéria orgânica, que redisponibiliza os nutrientes na sua forma inorgânica (Lalli & Parsons, 1997). Ademais, a fixação de nitrogênio molecular por alguns microrganismos pode contribuir na disponibilização de nitrato para o sistema (Dugdale & Goering, 1997; Reynolds et al., 2007).

Devido à grande demanda de macronutrientes inorgânicos pelos produtores primários, as camadas superficiais do oceano (eufóticas)

geralmente apresentam uma depleção suficiente para limitar produção primária em baixas e médias latitudes (Levitus *et al*., 1993). Em maiores profundidades, observamos maiores concentrações de macronutrientes, geralmente apresentando um máximo na região da termoclina. Nessa região, as partículas biogênicas sedimentantes formadas em superfície se acumulam, devido à barreira física de densidade e baixa advecção, fazendo com que a decomposição da matéria orgânica e redisponibilização dos nutrientes na forma inorgânica seja intensa (Libes, 2009).

Destoando do padrão oligotrófico da superfície das bacias oceânicas, encontramos as regiões de montes submarinos e ilhas oceânicas, onde podem ser observados aumentos das taxas de produtividade primária e biomassa em relação ao oceano adjacente. Este fenômeno foi descrito primeiramente por Doty & Oguri (1956) para uma ilha do Havaí e denominado como “efeito ilha” (*island mass effect*), sendo o processo equivalente para montanhas submarinhas denominado de “efeito monte submarino” (*seamount effect*). Mais tarde, o efeito foi documentado para diversas ilhas e montes submarinos ao redor do planeta (e. g. Sonnekus et al., 2017; Ma et al., 2019; Papiol et al., 2019). Gove et al. (2016) identificaram o efeito ilha em 91% dos atóis do oceano Pacífico, causando um aumento de 85,6% do estoque da biomassa de fitoplâncton em comparação ao oceano aberto adjacente.

Esse aumento da produtividade primária é explicado pelas maiores concentrações de nutrientes encontradas nos entornos de ilhas e montes submarinos, o que pode ser resultado de diversos fatores (resumidos na figura 1, Gove et al., 2016).

Regiões de montes e bancos submarinos, taludes continentais e ilhas são frequentemente relacionadas a intensas atividades hidrodinâmicas quando comparadas às planícies abissais, como resultado da interação destas feições com os escoamentos oceânicos (White et al., 2007). Estes processos incluem a formação de células de circulação sobre a feição topográfica (Lavelle & Mohn, 2010), elevação de isopicnais sobre a feição (Genin & Boehlert, 1985), aceleração de correntes (Lavelle & Mohn, 2010), amplificação de marés (Read & Pollard, 2017), formação e quebra de ondas internas (Toole et al., 1997), aumento da turbulência e mistura vertical de águas (Lueck & Mudge, 1997; Hasegawa et al., 2004), e formação de corredores de vórtices à sotacorrente da ilha em caso de correntes intensas (Heywood et al., 1990; Hasegawa et al., 2009).

Além dos fatores físicos citados anteriormente, para as ilhas oceânicas, os processos de aportes provenientes da própria ilha, tais como a lixiviação (Dandonneau & Charpy, 1985; Gove *et al*., 2016), a descarga de água subterrânea (Street *et al*., 2008), o descarte de efluentes (Gove et al., 2016) e o aporte pelas comunidades da própria ilha, contribuem no aporte de nutrientes e outros elementos para o oceano adjacente. Por exemplo, algumas ilhas oceânicas servem de berçário para espécies de aves, que acumulam nutrientes através de seus dejetos, sendo eventualmente disponibilizados para a região oceânica e afetando o ecossistema circundante (Kolb *et al*., 2010).

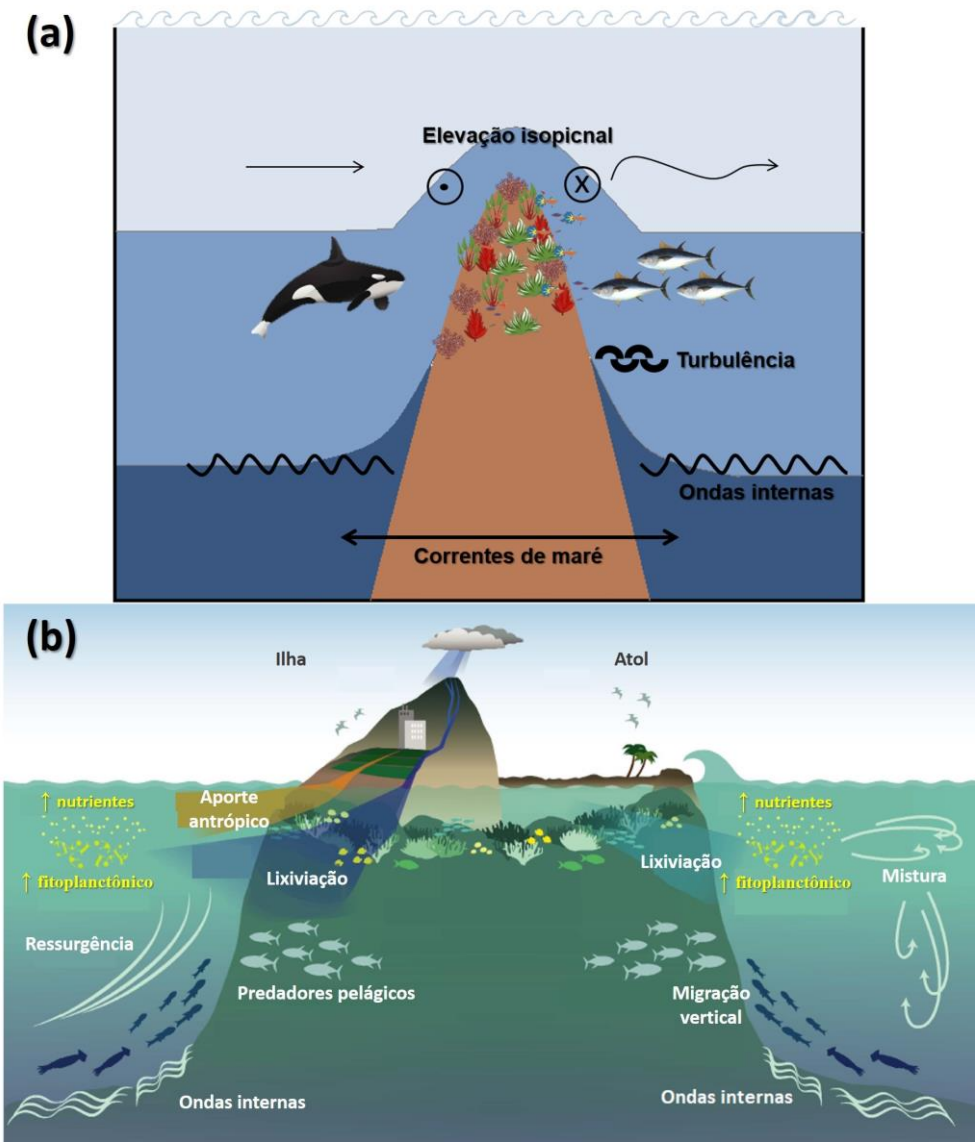

Figura 1: Processos associados ao: (a) efeito monte submarino; (b) efeito ilha (adaptado de Gove et al., 2016).

Como a produção primária constitui a base energética que sustenta toda a cadeia trófica dos oceanos, o aumento de nutrientes associado a feições topográficas forma um oásis de produção em meio a um oceano oligotrófico, com potencial para causar diversas consequências ecológicas (Rogers, 2018). Por exemplo, o aumento da biomassa fitoplanctônica sustenta uma maior biomassa de peixes planctívoros e piscívoros, que por sua vez é atrativo para

organismos nectônicos de maiores profundidades e predadores pelágicos, que migram para essas regiões em busca de alimento (Reid et al., 1991; McManus et al., 2008). Além disso, as cadeias de montes submarinos, como a de Vitória-Trindade no oceano Atlântico Sul, podem conectar populações de peixes recifais em períodos de variações do nível do mar, servindo como alpondras (Pinheiro et al., 2017).

Por conseguinte, montes submarinos e ilhas são ecossistemas únicos, altamente variáveis no espaço e no tempo, onde se encontra uma alta e abundante biodiversidade e endemismo. Ainda, estas feições estão presentes em todas as bacias oceânicas com estimativas de até mais de 130,000 ao redor do globo terrestre (Yesson et al., 2011).

Entretanto, apesar de sua importância ecológica e biogeoquímica, ainda são ecossistemas pouco estudados (Djurhuus et al., 2017). Sendo assim, esse trabalho apresenta uma contribuição para o conhecimento e discussão da região da Cadeia de montes submarinos e ilhas de Vitória-Trindade em relação ao efeito monte submarino, no qual são apresentadas as distribuições de macronutrientes inorgânicos dissolvidos, clorofila, oxigênio dissolvido, massas de água e propriedades hidrográficas da região.

1.1. Área de estudo

A Cadeia Vitória-Trindade é uma sequência linear de montes submarinos e ilhas localizadas no oceano Atlântico Sul, alinhada a leste com a cidade de Vitória (ES), entre as latitudes de 20º S e 21º S (figura 2). Estende-se desde o talude continental, 175 km da costa (38º W), até ao arquipélago de Trindade e Martin Vaz (29º W), 1140 km da costa (Almeida, 2007).

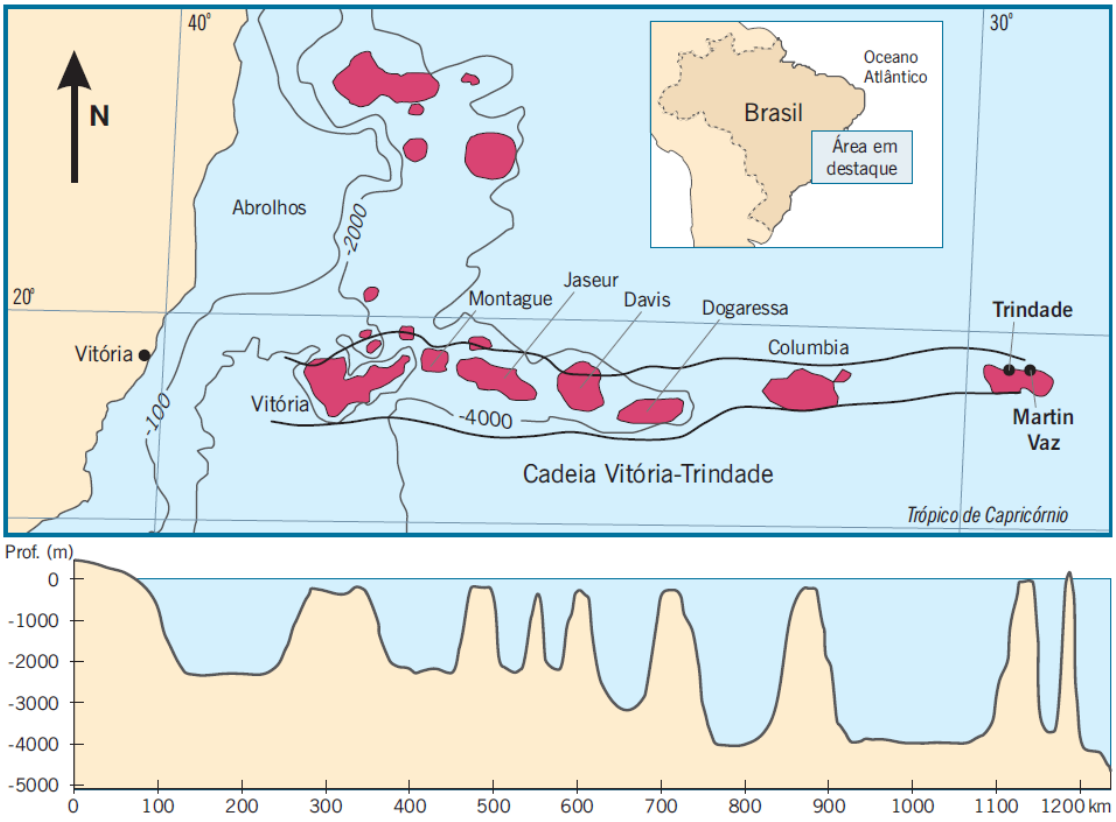

Figura 2: Localização e batimetria da região da Cadeia Vitória-Trindade. O painel inferior mostra um perfil esquemático da seção entre a região continental e o arquipélago de Trindade e Martim Vaz. Retirado de Almeida (2007).

A Cadeia Vitória-Trindade é constituída por aproximadamente 30 montes submarinos de forma cônica, caracterizados morfologicamente como edifícios vulcânicos (Motoki et al., 2012), compostos de rochas vulcânicas que são derivadas de picrobasaltos subalcalinos e com posterior formação de plataformas carbonáticas nos topos erodidos de paleovulcões (Skolotnev et al., 2010). Destes montes, 17 apresentam altura relativa superior a 2500 m, sendo os principais Vitória, Jaseur, Davis e Dogaressa, terminando no arquipélago de Trindade e Martim-Vaz (Motoki et al., 2012). Os dois primeiros têm aproximadamente 130 km de largura, com seus cumes a 60 m de profundidade, enquanto os dois últimos têm aproximadamente 50 km de

largura, com os cumes de 60 m e 150 m de profundidade, respectivamente (Lemos et al., 2018).

O clima da região é tropical oceânico com temperatura média anual de 25 °C, apresentando máximas de 30 °C em fevereiro e mínimas de 17 °C em agosto (Mohr et al., 2009). No verão a precipitação é intensa e periódica, o que é essencial para o abastecimento de lençol freático e cursos de água na Ilha Trindade, a única com fontes de água doce da cadeia (Alves, 1998). Entre abril e outubro, a ilha sofre efeitos de frentes frias periódicas procedentes da Antártica, que sobem pela Argentina e sul do Brasil e, ao chegarem à região Sudeste, seguem em direção ao oceano e atingem a ilha Trindade, provocando mudanças bruscas nas condições do mar (Durães et al. 2016).

A Cadeia Vitória-Trindade está localizada em uma região dinamicamente complexa do oceano Atlântico Sul. Entre 10º S e 20º S de latitude, um pouco ao norte da cadeia, a Corrente Sul Equatorial (SEC) se bifurca (Soutelino et al., 2011), dando origem a Corrente Norte do Brasil e a Corrente do Brasil, que flui para sul, bordejando o continente sul-americano (da Silveira et al., 2000). Na região dos bancos de Royal-Charlotte e de Abrolhos, a corrente do Brasil é defletida para nordeste, em direção ao oceano aberto, indo de encontro direto com a cadeia (Soutelino et al., 2011).

Através de análise geostrófica, Stramma (1990) estimou um transporte da Corrente do Brasil próximo a sua região de formação de 4 Sv (1 Sv = 10^6 m^3/s), onde é caracterizada por uma corrente rasa, quente e salina que carrega basicamente Água Tropical (da Silveira et al., 2000). A partir de 20°S, recebe contribuição da Água Central do Atlântico Sul, quando se torna mais profunda e

cresce em transporte (da Silveira et al., 2000). Em 20,3°S, a Corrente do Brasil se encontra com a barreira topográfica da Cadeia Vitória-Trindade, quando acaba por fluir entre os canais dos montes submarinos mais próximos ao talude continental (Evans et al., 1983). Os transportes obtidos para a região foram de aproximadamente 4 Sv, relativamente ao nível de 500 db (Evans & Signorini, 1985).

Abaixo da picnoclina, a Corrente de Contorno Oeste Intermediária flui na direção oposta à Corrente do Brasil na área de estudo, carregando a Água Intermediária Antártica para o norte através da Cadeia Vitória-Trindade (Soutelino et al., 2013). A Cadeia Vitória-Trindade também marca a latitude de bifurcação da Água Central do Atlântico Sul (Stramma e England, 1999). Portanto, ao norte dessa latitude, a Água Central do Atlântico Sul flui para o norte, adicionando transporte à Corrente de Contorno Oeste Intermediária e iniciando um fluxo que se torna a Contracorrente Norte Equatorial (Soutelino et al., 2013). Em níveis mais profundos, a Corrente de Contorno Oeste Profunda leva a Água Profunda do Atlântico Norte para o sul (Soutelino et al. 2013). Este padrão de circulação e distribuição de massas de água ao longo da porção oeste do oceano Atlântico Sul encontra-se representado na figura 3.

Outra característica interessante da região de estudo é a presença de um vórtice de núcleo frio e de baixa salinidade, o Vórtice de Trindade, localizado ligeiramente ao sul da Cadeia Vitória-Trindade, o qual é formado pela interação entre a Corrente do Brasil, o talude continental e a topografia local (Schmid et al., 1995). Na superfície do vórtice, Gaeta et al. (1999) encontraram de 1 a 2 concentrações mais altas de clorofila do que nas áreas

vizinhas, revelando a importância do vórtice para a produção primária no Atlântico Subtropical.

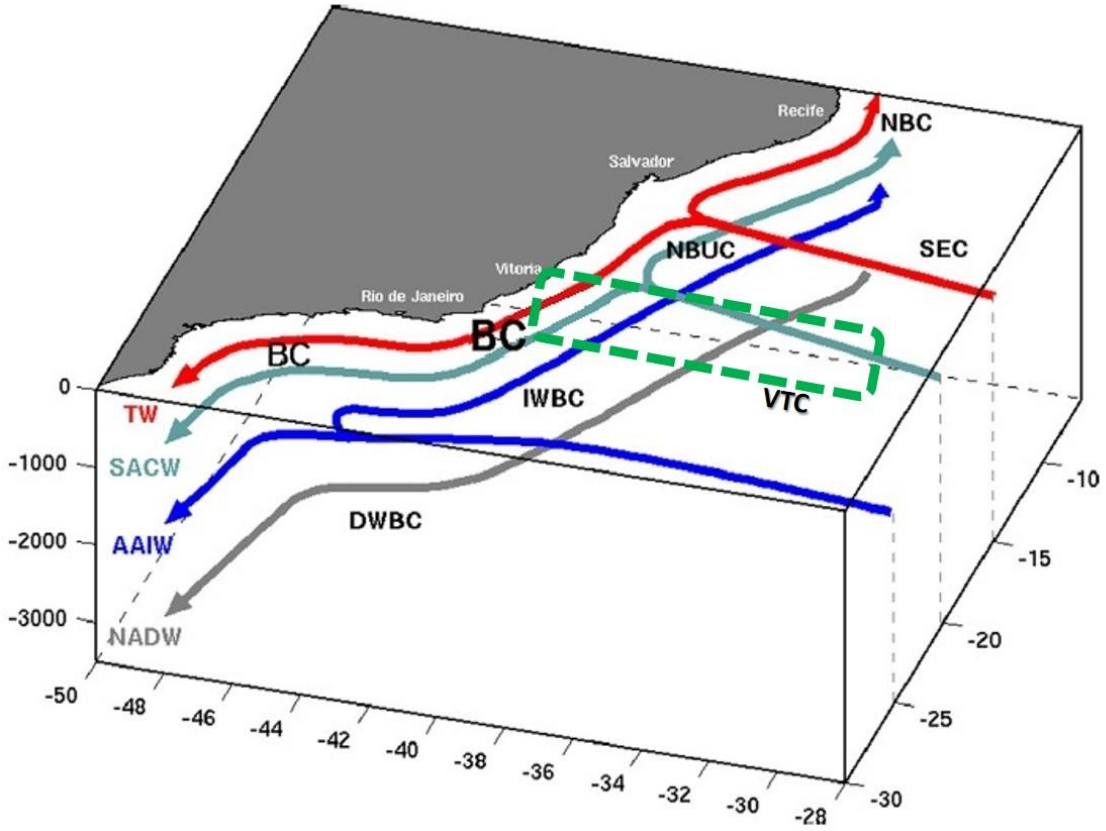

Figura 3: Esquema de circulação oceânica para a região de estudo. A região delimitada pelo quadro verde indica a localização da Cadeia Vitória-Trindade (VTC). SEC: Corrente Sul Equatorial; BC: Corrente do Brasil; NBC: Corrente Norte do Brasil; NBUC: Contracorrente Norte Equatorial; IWBC: Corrente de Contorno Oeste Intermediária; DWBC: Corrente de Contorno Oeste Profunda; TW: Água Tropical; SACW: Água Central do Atlântico Sul; AAIW: Água Intermediária Antártica; NADW: Água Profunda do Atlântico Norte. Adaptado de Soutelino et al. (2013).

A Cadeia Vitória-Trindade também é uma região de riqueza biológica. Através da análise de dados de satélite, Lemos et al. (2018) encontraram que na região da Cadeia Vitória-Trindade ocorrem florações sazonais,

principalmente nos meses de inverno. Além disso, a região já foi reportada como sendo um *hotspot* de abundância de bactérias (Andrade et al., 2004) biodiversidade e alto endemismo de peixes (Pinheiro et al., 2015). Esta abundância bacteriana e de flora/fauna marinha têm sido parcialmente associada à presença de extensas áreas de rodolitos (Amado-Filho et al., 2007; Pereira-Filho et al., 2012), que são o tipo de fundo predominante na região dos cumes dos montes submarinos da cadeia, das regiões insulares e da plataforma continental (Meirelles et al., 2015).

Capítulo II:

Objetivos

2. Objetivos

2.1. Geral

Investigar a distribuição dos macronutrientes inorgânicos dissolvidos e massas de água, bem como suas interações com variáveis físicas e químicas na região da Cadeia Vitória-Trindade, localizada no oeste do oceano Atlântico Sul.

2.2. Específicos

- A partir dos parâmetros físicos e químicos, identificar as massas de água locais, bem como suas distribuições.
- Estimar o impacto da remineralização da matéria orgânica na distribuição vertical dos macronutrientes na área de estudo.
- Avaliar o efeito monte submarino na fertilização das águas oligotróficas na região da Cadeia Vitória-Trindade.

Capítulo III:

Resultados e Discussões

Para a obtenção do título de Mestre pelo Programa de Pós-Graduação em Oceanologia, é requerido que o discente realize a submissão de pelo menos um artigo científico como primeiro autor em periódico com corpo indexado. Desse modo, os resultados da pesquisa desenvolvida durante o período de mestrado e a discussão dos resultados serão apresentados em forma de artigo neste Capítulo. O manuscrito, de autoria de Elis Brandão Rocha, Eunice da Costa Machado, Gabriel Karagiannis de Souza, Kayla Correa de Lima, Paulo Henrique Rezende Calil e Carlos Francisco Ferreira de Andrade, é intitulado "**The controls of water masses and topographic features on inorganic macronutrient and chlorophyll distributions in the oligotrophic Vitoria-Trindade Chain region, Southwestern Atlantic Ocean**" e foi submetido para publicação no periódico "*Journal of Marine Systems"*.

The controls of water masses and topographic features on inorganic macronutrient and chlorophyll distributions in the oligotrophic Vitoria-Trindade Chain region, western South Atlantic Ocean

Elis Brandão Rocha[1]*, Eunice da Costa Machado[1], Gabriel Karagiannis de Souza[1], Kayla Correa de Lima[2], Paulo Henrique Rezende Calil[3] and Carlos Francisco Ferreira de Andrade[1]

[1] Instituto de Oceanografia, Laboratório de Hidroquímica, Universidade Federal do Rio Grande, Rio Grande, RS, Brazil.

[2] Laboratório de Etnoconservação e Áreas Protegidas, Universidade Estadual de Santa Cruz, Ilhéus, BA, Brazil.

[3] Institute of Coastal Research, Helmholtz-Zentrum, Geesthacht, Germany.

*Corresponding author:
E-mail address: elis.brandao@gmail.com

1. Introduction

Phytoplankton production is an essential source of energy in the marine environment, which sustains the trophic structure of the entire marine ecosystem (Duarte and Cebrián, 1996). Its production in the ocean, however, is mostly limited by availability of dissolved inorganic macronutrients and light. Oceanic regions in tropical zones are usually considered oligotrophic, due to minimal vertical flow of nutrients to the euphotic zone and, consequently low biological productivity (Louanchi and Najjar, 2000). This configuration is explained by the presence of a warm surface layer above a colder and denser subsurface layer, creating a permanent thermocline. This physical barrier prevents the upward flow of deeper nutrient-rich layers, constraining the primary production in the surface waters (de Souza et al., 2013).

Nevertheless, the interaction between the ocean's dynamic and topographic features, such as seamounts, may have a great impact on the oligotrophic pattern of a region. Seamounts are ubiquitous features of the

world's underwater topography, with estimates of as many as 33,452 and reaching 1000 m higher than the seafloor (Yesson, 2011). However, their biogeochemistry is still poorly known (Djurhuus et al., 2017). They are important since they seem to support relatively higher rates of primary productivity, and, consequently, larger benthic and consumers biomass than the surrounding ocean (Clark et al., 2010), a phenomenon referred to as "island-mass effect" or "seamount effect". This is explained by the increase of inorganic macronutrients in the euphotic zone, as a result of a perturbation of the oceanic flows, therefore, enhancing turbulence and mixing (Lueck and Mudge, 1997), raising internal tides (Read and Pollard, 2017), promoting isopycnal uplifting, such as Taylor Caps (Genin and Boehlert, 1985; de Souza et al., 2013) and providing a source of eddy formation (Arístegui et al., 1994; Hasegawa et al., 2009).

In this context, this paper is placed under the framework of the multidisciplinary project "Can an Archipelago Fertilize the Ocean?" that aims to understand the seamount/island-mass effect in the region of the Vitória-Trindade Chain (VTC), located in the western South Atlantic Ocean (SAO). The VTC is a linear sequence of seamounts and islands lined up eastward with the city of Vitória (Brazil), between the latitudes of 20º S and 21º S. It extends from the continental slope, 175 km from the shore (38º W), until the Trindade and Martin Vaz archipelago (29º W), 1140 km from the shore (Almeida, 2007).

The approximately 30 seamounts of the VTC have a conical shape, morphologically characterised as volcanic edifices (Motoki et al.,2012), composed of volcanic rocks that are the derivatives of subalkaline picrobasalts with posterior formation of carbonate platforms on the eroded tops of the paleovolcanoes (Skolotnev et al., 2010). Of these features, 17 present a relative height superior to 2500 m, the main ones being Vitória, Jaseur, Davis and Dogaressa, ending at the Trindade and Martim-Vaz archipelago (Motoki et al., 2012). The first two are approximately 130 km wide with their summits 60 m deep, whereas the latter two are approximately 50 km wide with summits 60 m and 150 m deep, respectively (Lemos et al., 2018).

The VTC is located in a complex and dynamically relevant region of the SAO, standing as a barrier to the passage of the western boundary current

system. The upper layer circulation is dominated by the anticyclonic subtropical South Atlantic gyre. Around 10° and 20° S, north of the VTC, the South Equatorial Current (SEC) divides itself (Soutelino et al., 2011), originating the North Brazil Current (NBC) and the Brazil Current (BC), which flows southward, bordering the South-American shelf (da Silveira et al., 2000). When in the region of the Royal-Charlotte and Abrolhos banks, the BC moves offshore and northeastward, flowing directly towards the VTC (Soutelino et al., 2011). The VTC also marks the latitude of bifurcation of westward South Atlantic Central Water (SACW) flow. Thus, south of this, the SACW adds transport to the BC. At the intermediate level, the Intermediate Western Boundary Current (IWBC) flows in the opposite direction to the BC, carrying the Antarctic Intermediate Water (AAIW) northwards through the VTC (Soutelino et al., 2013). At deeper levels, the North Atlantic Deep Water (NADW) formed in the northern hemisphere is carried southwards as a Deep Western Boundary Current - DWBC (Soutelino et al. 2013).

Another interesting feature of the study region is the presence of a cold and low salinity cyclonic eddy (referred to as Vitória Eddy), located south of the VTC. The Vitória Eddy is formed by the interaction between the BC, the shelf break and the local topography (Schmid et al., 1995). On the surface of the inner core of the eddy, Gaeta et al. (1999) found chlorophyll concentrations 1 to 2-fold higher than in the surrounding areas, revealing its importance to the primary production in the Subtropical Atlantic.

In addition to the hydrodynamic complexity, the presence of the VTC is associated with biological richness. Lemos et al. (2018) found higher surface chlorophyll concentrations associated to the VTC seamounts via analysis of satellite derived data. As a consequence, the VTC is a hotspot of bacterial abundance (Andrade et al., 2004) and primary productivity (Gaeta et al., 1999), and contains concentrations of large stocks of commercially important fish (Pinheiro et al., 2015). The richest bacterial abundance, marine flora and its diversity have been partly associated with the presence of extensive areas of rhodoliths (Amado-Filho et al., 2007; Pereira-Filho et al., 2011), which is the

predominant bottom type at the VTC seamount summits and outer insular shelves (Meirelles et al., 2015).

During the Recursos Vivos da Zona Econômica Exclusiva (REVIZEE) Program, higher surface concentrations of inorganic macronutrients were reported in the VTC when compared to other Brazilian oceanic areas (Rezende et al., 2006; Braid, 2008), but the sampling was only carried out to a depth of 200 m of the water column. In order to further understand and place subsequent investigation related to the seamount/island mass effect in the VTC, as a first step this paper discusses, in general terms, the distribution of inorganic macronutrients, dissolved oxygen and chlorophyll in relation to the VTC seamounts. It also describes the distribution of water masses present in the region from the surface to a depth of 3000 m in the water column.

2. Materials and Methods

2.1. Data sampling and handling

Data were collected on board the RV Alpha Crucis from the São Paulo University. Sampling were taken between 27th of January and 15th of February 2017, through two sections perpendicular to the coast. One of them was over the VTC (section A) and the other was south of the chain (section B, figure 1).

A total of 43 oceanographic stations were profiled for salinity, temperature and pressure through the use of a CTD (Sea-Bird SBE 911) equipped with dissolved oxygen (SBE 43) and Chl-a 123 fluorescence (Turner Cyclops 2) sensors (blue and red dots in figure 1). The sensors were calibrated within a period of 6 months prior to the cruise. Data-gathering depths reached the 3000 m along section A and 1000 m along section B. In 33 of these stations, 266 water samples were collected for the determination of pH and inorganic macronutrients (phosphate - PO_4^{-3}, nitrate - NO_3^- and dissolved inorganic silica - DSi) using 12 L Niskin bottles (red dots, Figura 1). The depths chosen for the discrete sampling were set considering the depths of the permanent thermocline, oxygen minimum zone and chlorophyll maximum zone.

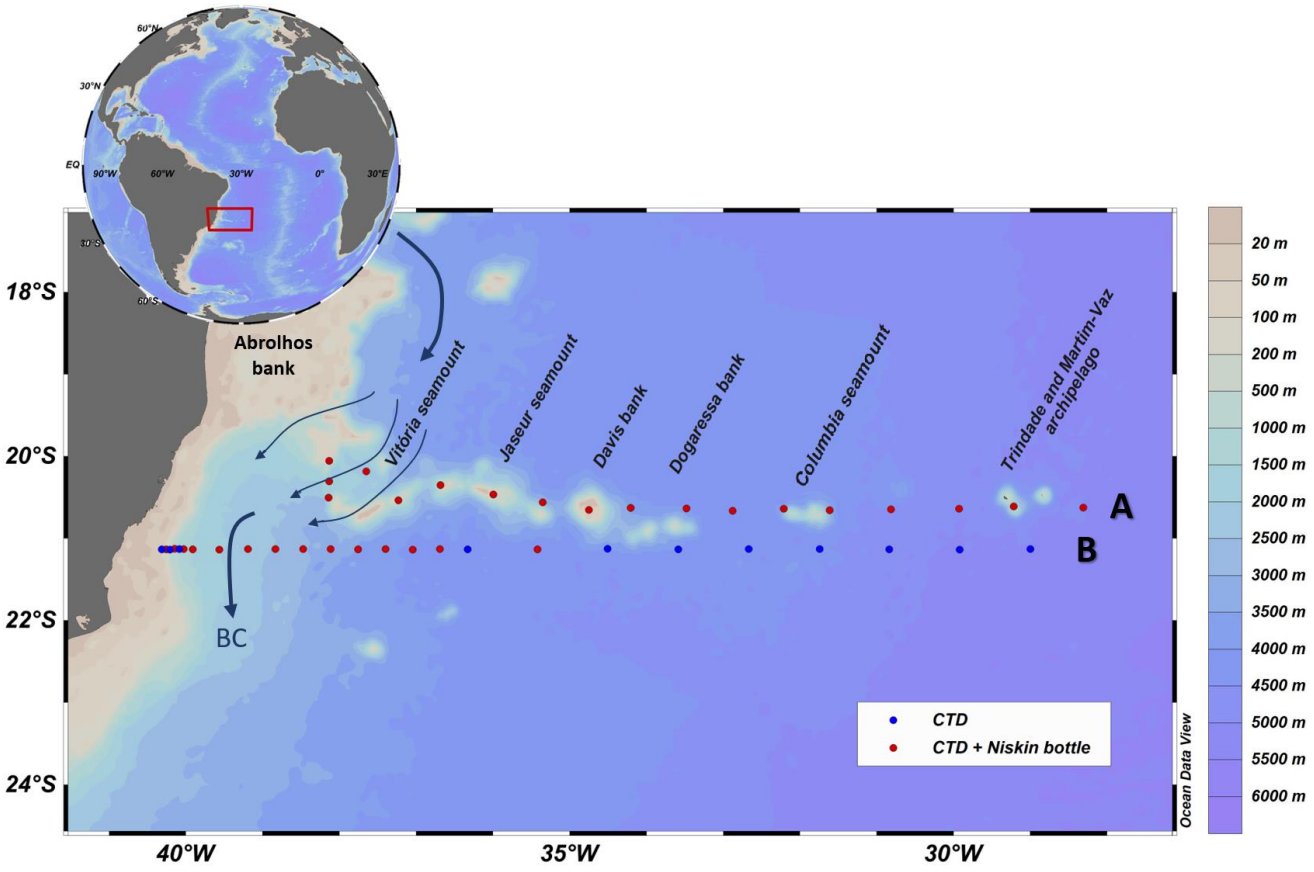

Figure 1: Location of the stations in sections A and B along the study area. The location of the main topographic features in the region are shown. The blue dots represent the CTD stations and the red dots represents the stations where chemical analyses of seawater were carried out. The blue arrows indicate the pathway of the Brazil Current (BC) in the study area (Evans et al., 1983).

For the analysis of dissolved inorganic macronutrients, the samples were filtered onboard through 0.2 µm cellulose acetate filters and preserved through freezing (-20°C). The samples were thawed at laboratory temperature for the colorimetric analysis under a spectrophotometer using 10, 5 or 1 cm light path cells depending on the concentration of the sample (Aminot and Chaussepied, 1983). Accuracy of analytical results was checked by analysing a certified reference material (CRM), the SCOR-JAMSTEC WG 147 for the Atlantic water (Low in Atlantic, Kanso Lot. CE). The limits of detection and quantification were calculated based on at least 10 blanks following The International Union of Pure and Applied Chemistry - IUPAC (Christian, 2004) (table 1). The nitrate concentration of the CRM was not detected in our analyses, since it presents

lower concentrations than the detection limit. Despite that, we are confident concerning the results, as the routine analysis is carried by checking prepared standards of analytical grade and by following an analytical control chart.

Table 1: Concentration of inorganic macronutrients in the Certified Reference Material SCOR-JAMSTEC WG 147 (CRM), measured concentration of the CRM, detection limit and quantification limit given in µmol/kg.

	CRM's concentration	**CRM's measured concentration**	**Detection Limit**	**Quantification Limit**
Phosphate	0.012±0.006	0.011	0.010	0.031
Nitrate	0.010±0.03	n.d.(*)	0.26	0.87
Silicate	0.060±0.09	0.095	0.045	0.120

(*)not detected.

The pH samples were analysed on board, immediately after the water sampling. pH was potentiometric determined through a Digimed DM- 22 pH meter coupled with a glass-reference electrode cell and a temperature sensor. The sensors were calibrated with buffer solutions with pH values equal to 4.01 (Digimed DM-S1A) and 6.86 (Digimed DM-S1B), both at 25ºC, before the samples of each profile were measured

The surface Mixed Layer Depth (MLD) was calculated following Monterey and Levitus (1997). It was based on fixed differences of 0.5 °C in potential temperature and 0.125 kg/m^3 in potential density from a reference of a depth of 10 m. All figures and maps presented in this study were elaborated using the freely available software Ocean Data View (Schlitzer, 2017; odv.awi.de).

2.2. The extended Optimum Multiparameter (eOMP) analysis

We used the extended Optimum Multiparameter analysis (eOMP) to identify the relative contribution of water masses along the two sections in the

VTC. The method was proposed by Tomczak (1981) and updated by Tomczak and Large (1989). It is a water mass inverse model based on solving over-determined linear equations to find the relative contributions of different source water types (SWTs, or end-members) that best reproduce the observed data, while the residuals are minimised by applying a non-negative least squares method. The extended version was proposed later by Karstensen and Tomczak (1997), who included the stoichiometric ratios of organic matter remineralisation to account for the non-conservative behavior of oxygen and inorganic macronutrients, allowing the application at oceanic scales. The basic structure of eOMP analysis is written as:

$$
\begin{aligned}
x_1\,T_1 + \ldots + x_6\,T_6 \qquad\qquad - T_{obs} &= R_T,\\
x_1\,S_1 + \ldots + x_6\,S_6 \qquad\qquad - S_{obs} &= R_S,\\
x_1\,O_1 + \ldots + x_6\,O_6 - r\,{}^{O}/_{P} - O_{obs} &= R_O,\\
x_1\,Si_1 + \ldots + x_6\,Si_6 + r\,{}^{Si}/_{P} - Si_{obs} &= R_{Si},\\
x_1\,P_1 + \ldots + x_6\,P_6 + \quad 1 \quad + P_{obs} &= R_P,\\
x_1\,N_1 + \ldots + x_6\,N_6 + r\,{}^{N}/_{P} - N_{obs} &= R_N,\\
x_1 + \ldots + x_6 - 1 &= R_{MC}.
\end{aligned}
$$

Where x_i (i=1-6) is the relative fraction (or contribution %) of n SWTs; T_i, S_i, O_i, Si_i, P_i and N_i represent, respectively, the temperature, salinity, dissolved oxygen, dissolved silica, phosphate and nitrate+nitrite parameters of the n SWTs; T_{obs}, S_{obs}, O_{obs}, Si_{obs}, P_{obs} and N_{obs} stand for the observed parameters data; the $r_{O/P}$, $r_{Si/P}$, $r_{N/P}$ are the stoichiometric ratios of remineralisation, all referenced to phosphate; and column R represents residue from the eOMP calculation for each parameter. The last line represents the mass conservation equation of the system. Therefore, the number of hydrographic properties available from observations restricts the number of SWTs in the water masses analysis, that should be n-1, or else the system becomes underdetermined (Tomczak and Large, 1989; Poole and Tomczak, 1999).

The main advantage of eOMP analysis is related to few assumptions: (i) a water mass can be fully represented by the combination of determined SWTs and (ii) the sum of the contributions should be 100% and non-negative, obeying

the law of mass conservation. Therefore, the first step is to select which SWT will define a sample, and what are their physical and chemical characterisation. The water masses that compose the water column of the study region were analysed based on the TS diagram, location and descriptions of water types in the literature (Stramma and England, 1999; Memery et al., 2000; Álvarez et al., 2014), and were the subject of this analysis: the Tropical Water (TW), South Atlantic Central Water (SACW), Antarctic Intermediate Water (AAIW), North Atlantic Deep Water (NADW) and Antarctic Bottom Water (AABW). Figure 2 shows the relation between the defined SWTs, described below, and the TS diagram with the whole set of samples.

TW is characterised by a warm, high salinity and oligotrophic water mass that is formed in the tropical region in both hemispheres (Stramma and England, 1999). It is also known as a Salinity Maximum Water, which is located in the upper 200 m in the water column, formed between 12° and 22° S, as observed in the World Ocean Circulation Experiment (WOCE) A17 transect data by Memery et al. (2000). Thus, the TW's thermohaline definition was taken from Álvarez et al. (2014) and the chemical characterisation was taken from stations between 14° and 16°S of the WOCE A17 transect, within the formation region of the water mass.

The chosen SWT definition for the SACW was the Western South Atlantic Central Water proposed by Poole and Tomczak (1999) (here defined as the $SACW_{upper}$ and $SACW_{lower}$), which was evaluated based on vertical/horizontal sections in the World Ocean Atlas dataset in the vicinity of its formation region, near the Brazil-Malvinas Confluence region of the Subtropical Convergence (Sprintall and Tomczak, 1993). The standard deviation of the SWT definition for SACW was taken from Liu and Tanhua (2019).

The definitions for the AAIW and AABW were taken from de Carvalho Ferreira and Kerr (2017), which were determined in the respective formation region with the dataset available in the 2013 World Ocean Database. The AABW defined here is its warmer and lowest density variety formed in the Weddell Sea, the Weddell Sea Deep Water (WSDW), since Brazil's abyssal basin is predominantly (up to 80%) composed of WSDW. The denser variety,

Weddell Sea Bottom Water (WSBW), is topographically constrained and remains trapped in the ridges close to 60°S (de Carvalho Ferreira and Kerr, 2017).

North Atlantic Deep Water is carried to the SAO by the DWBC (Garzoli et al., 2015). According to Álvarez et al. (2014) and Brea et al. (2004), NADW is split into two SWTs: $NADW_{upper}$, which corresponds to the contributions of the Mediterranean Water and Labrador Sea Water; and $NADW_{lower}$, relating the contributions of the overflow spill in the Denmark Strait and Iceland-Scotland sills. The SWT definition of the $NADW_{upper}$ was taken from the northern end of the Woce A17 transect (Álvarez et al., 2014; Brea et al., 2004). The $NADW_{lower}$ was taken from Lee et al. (2003), which was determined in 44°N through the analysis of a combined dataset collected between 1990 and 1998 as part of WOCE Hydrographic Program, the Joint Global Ocean Flux Study (JGOFS), and the Ocean-Atmosphere Carbon Exchange Study (OACES). The Upper Circumpolar Deep Water (UCDW) is also found in the realm of deep water masses in the SAO (Stramma and England, 1999), but it was not studied here since Álvarez et al. (2014) verified that its contribution was minimal (less than 30%) north of 26°S. Furthermore, the authors concluded that north of 23°S the AAIW is the dominant water mass at the UCDW maximum.

A total of 6 parameters (T, S, O, P, N e Si), measured from the Niskin bottles, were considered in the analysis, thus a total of 5 SWTs can be analysed in the eOMP. Since a mixture of 7 SWTs in the water column of the study region was considered, the first step was to break the analysis into vertical domains according to the potential density: (i) upper (potential density smaller/equal than 27.05 kg/m^3) which includes the TW, $SACW_{upper}$, $SACW_{lower}$, AAIW and $NADW_{upper}$; and (ii) lower (potential density greater than 27.05 kg/m^3), which includes the $SACW_{lower}$, AAIW, $NADW_{upper}$, $NADW_{lower}$ and AABW (figure 2). For the upper domain, no contribution of AABW was considered. Also, no contribution of TW was considered for the lower domain. In addition, data with potential density smaller than 24.5 kg/m^3, basically the first 50 m of the water column (which is approximately the depth of the MLD), were removed because

of the interaction of this layer with the atmosphere and consequently non conservative behaviour of its proprieties.

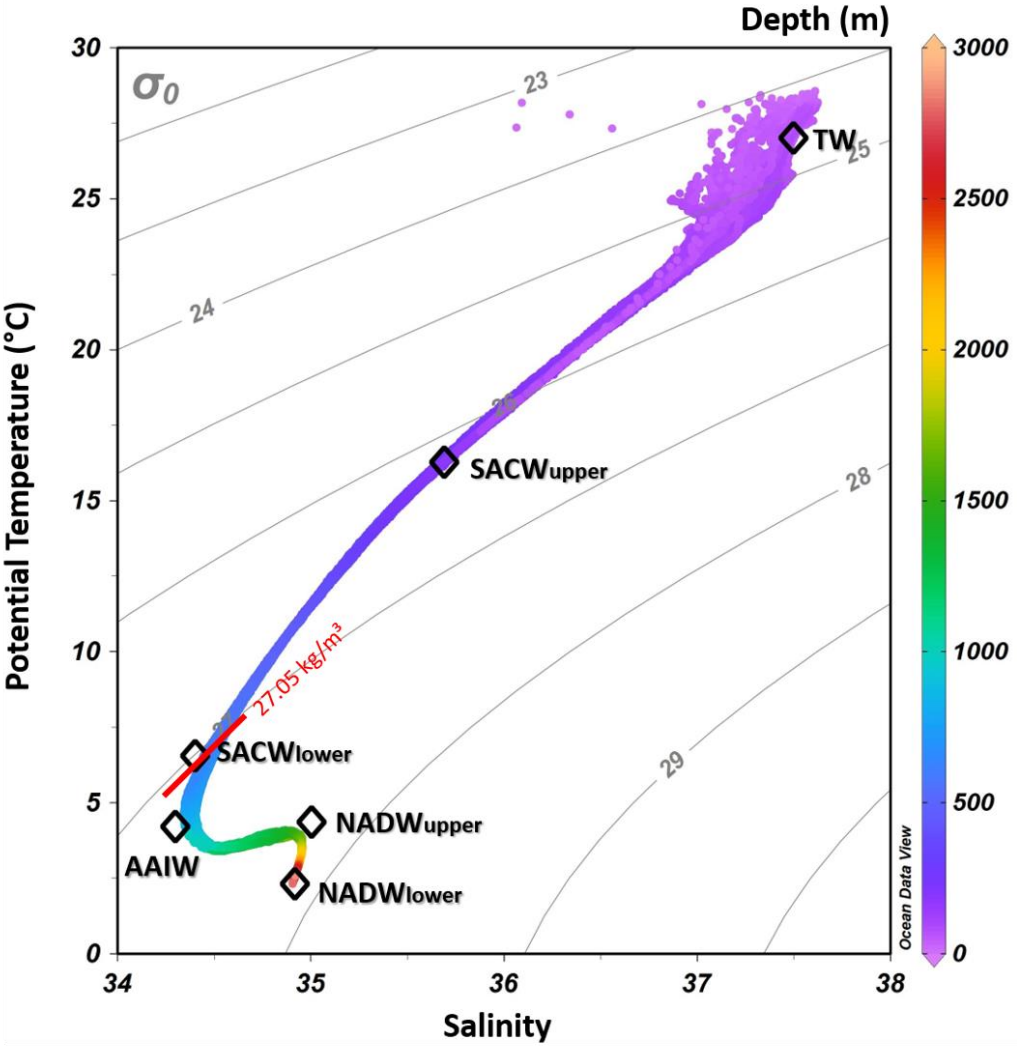

Figure 2: Potential temperature (°C)/salinity diagram for all the sampled stations. Black diamonds represent the SWT definitions used in the eOMP analysis. The red line indicates the potential density (27.05 kg/m³) in which the eOMP analysis was divided in upper and lower domains. The colourbar shows the sampling depths. Isopycnals are presented as light grey lines.

The eOMP also requires weighting the parameters of the analysis. Several weights were tested and it was chosen the ones that presented the least amount of mass conservation residue. The weights used were: 24, 24, 2,

2, 1, 2 and 100 for T, S, O, P, N, Si and mass conservation, respectively. The stoichiometric ratios of remineralisation of organic matter used were the ones proposed by Anderson and Sarmiento (1994), except for the $R_{Si/P,}$ which was proposed by Poole and Tomczak (1999). Sensitivity tests were performed by analysing the same dataset by adding and subtracting the standard deviation (extracted from the literature) from all parameters that defined the SWTs, according to de Souza et al. (2018) and de Carvalho Ferreira & Kerr (2017). Only the results with residuals lower than 5% were used. The results presented in this paper are the average contribution of all the eOMP runs performed. Table 2 summarises the SWTs, their standard deviations and ratios used in the analysis.

Table 2: Source water type (SWT) indices and standard deviations for T (potential temperature - °C), S (salinity), O (dissolved oxygen - µmol/kg), P (phosphate - µmol/kg), N (nitrate+nitrite - µmol/kg) and Si (silicate - µmol/kg); stoichiometric ratios of remineralisation of organic matter and references.

SWT	T	S	O	P	N	Si	Reference
TW	27±0.1	37.5±0.01	198.5±1.09	0.106±0.01	0.04±0.001	1.01±0.14	Woce A17 – Memery et al. (2000); Álvarez et al. (2014)
$SACW_{upper}$	16.27±2.02	35.69±0.32	239.57±6.2	0.20±0.24	0±3.6	1.68±0.99	Poole and Tomczak (1999); Liu and Tanhua (2019)
$SACW_{lower}$	6.55±2.02	34.40±0.32	295.41±6.2	1.11±0.24	13.33±3.6	4.11±0.99	Poole and Tomczak (1999); Liu and Tanhua (2019)
AAIW	4.2±0.01	34.3±0.01	233±3	2±0.03	28.8±0.5	31±0.3	de Carvalho Ferreira and Kerr (2017)
$NADW_{upper}$	4.35±0.13	35.006±0.005	237.26±6.56	1.34±0.04	20.47±0.6	16.54±0.61	Woce A17 – Álvarez et al. (2014); Brea et al. (2004)
$NADW_{lower}$	2.3±0.38	34.92±0.03	263.62±14.99	1.24±0.15	18.52±2.31	26.64±11.41	Lee et al. (2003)
AABW	0±0.005	34.67±0.005	217±3	2.34±0.04	33.8±0.6	125±2	de Carvalho Ferreira and Kerr (2017)
Stoichiometric ratio	n/a	n/a	-170	1	16	10.3	Anderson and Sarmiento (1995); Poole and Tomczak (1999)

2.3. The remineralisation of dissolved inorganic macronutrients

Consumption and remineralisation of dissolved inorganic macronutrients by marine organisms often occur in ratios that differ from the ratios of the observed concentrations of those macronutrients in the surrounding ocean (Fanning, 1992). Hence, we attempted to calculate the remineralisation ratios of organic matter following the method proposed by Takahashi et al. (1985), which is based on the differences between preformed and observed concentrations of inorganic macronutrients and dissolved oxygen on determined isopycnals. In this method, the chemical preformed characterisation of the water masses is established through linear extrapolation of property-oxygen trends to oxygen saturation. However, the method has the disadvantage that only a mixture of two SWT can be used in the calculation, which is hardly a real scenario for our study region. In addition, we were unable to acquire approximately linear relationships between our chemical data and, thus, determine our preformed variables.

Therefore, a second approach was taken, following the method proposed by Li et al. (2000). This method is also based on a two end-member mixing, but it has the advantage that it is not necessary to determine preformed variables of water masses, as the definition of preformed conditions may introduce additional uncertainties. Instead, it applies a multiple linear regression of dissolved oxygen, nitrate (or phosphate) and potential temperature to directly determine the molar ratios of the consumed dissolved oxygen in relation to remineralised nitrate (R_N) or phosphate (R_P). Once R_N and R_P are known, it is possible to calculate the preformed nitrate and phosphate of any water sample by relating it to the Apparent Oxygen Utilization (AOU). This is the difference of the saturated dissolved oxygen concentration (at a given temperature and salinity) and the measured dissolved oxygen in the sample. Unfortunately, once again, the method was not suitable for our analysis, since we were unable to determine a correlation between our potential temperature, dissolved oxygen and inorganic macronutrients, which led to unrealistic values of R_N and R_P. This problem was likely due to the relatively low number of sampled stations and the

high variability in the dissolved oxygen data in our study region, as exemplified by figure 7.

For that reason, we estimated the amount of remineralised inorganic macronutrients in each water mass, as determined by the eOMP analysis, by relating the remineralisation ratios proposed by Anderson and Sarmiento (1994) and Guglielmi et al. (2017) and the AOU. The first considers a constant ratio of remineralised nitrate and phosphate in relation to dissolved oxygen to the entire water column, while the second proposes varying ratios for different depths and regions of the Atlantic Ocean. Here, it was chosen the ratios for the region between 20°S-45°S in the western SAO.

3. Results and Discussion

3.1. Distribution of hydrographic properties and water masses

Figures 3, 4 and 5 are plots of the potential temperature, salinity and dissolved oxygen, respectively, as measured by the CTD sensors for sections A and B. The plots consist of two panels separated by scale of depth in order to better resolve the upper layer of the water column. The top panels show the first 200 m of the water column in expanded scale, while the bottom panels show the entire sampled water column (0 - 3000 m, for section A, and 0 – 1000 m, for section B). The along-track bottom topography shown in the figures as a dark grey mask was the General Bathymetric Charts of the Ocean (GEBCO), 2014, 6v6. Names of topographic features are indicated in figure 3 for section A. Also, the figures show the MLD plotted as a dashed black line.

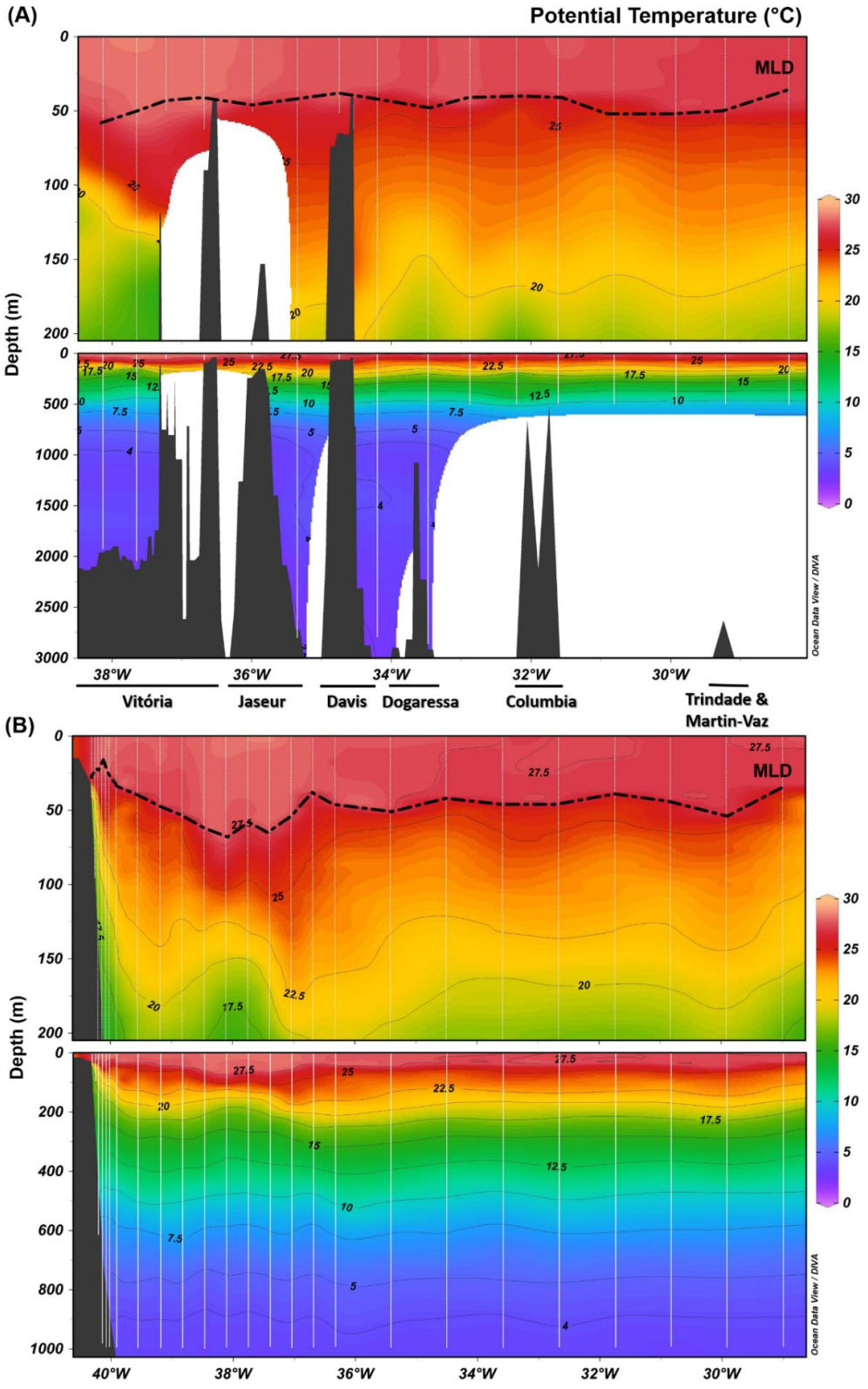

Figure 3: Distribution of potential temperature (°C) for (A) section A; and (B) section B. The mixed layer depths (MLD) are indicated as a black dashed line. The VTC main topographic features names are indicated at the bottom of figure section A. White lines indicate station location.

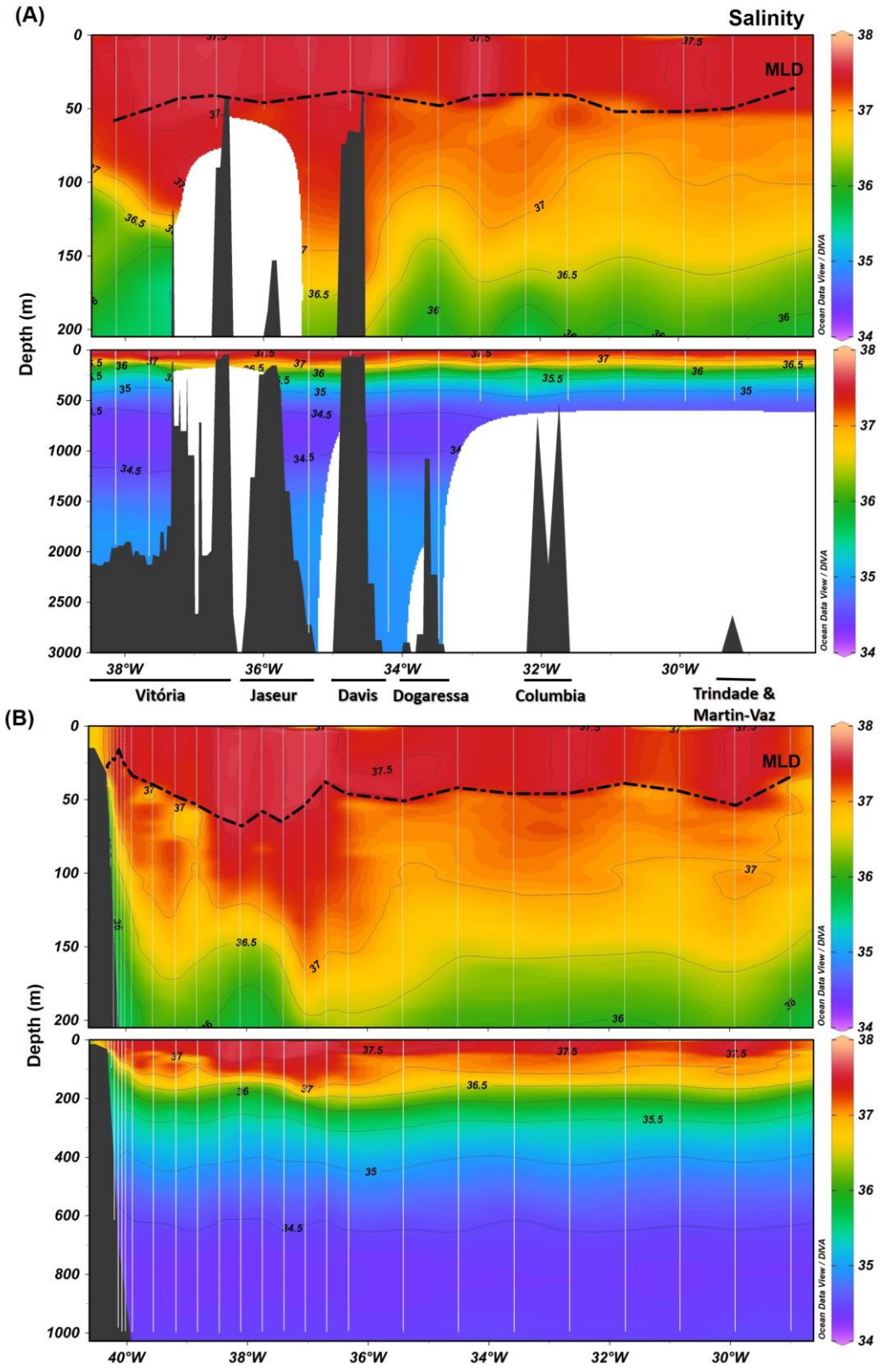

Figure 4: Distribution of salinity for (A) section A; and (B) section B. The mixed layer depths (MLD) are indicated as a black dashed line. The VTC main topographic features names are indicated at the bottom of figure section A. White lines indicate station location.

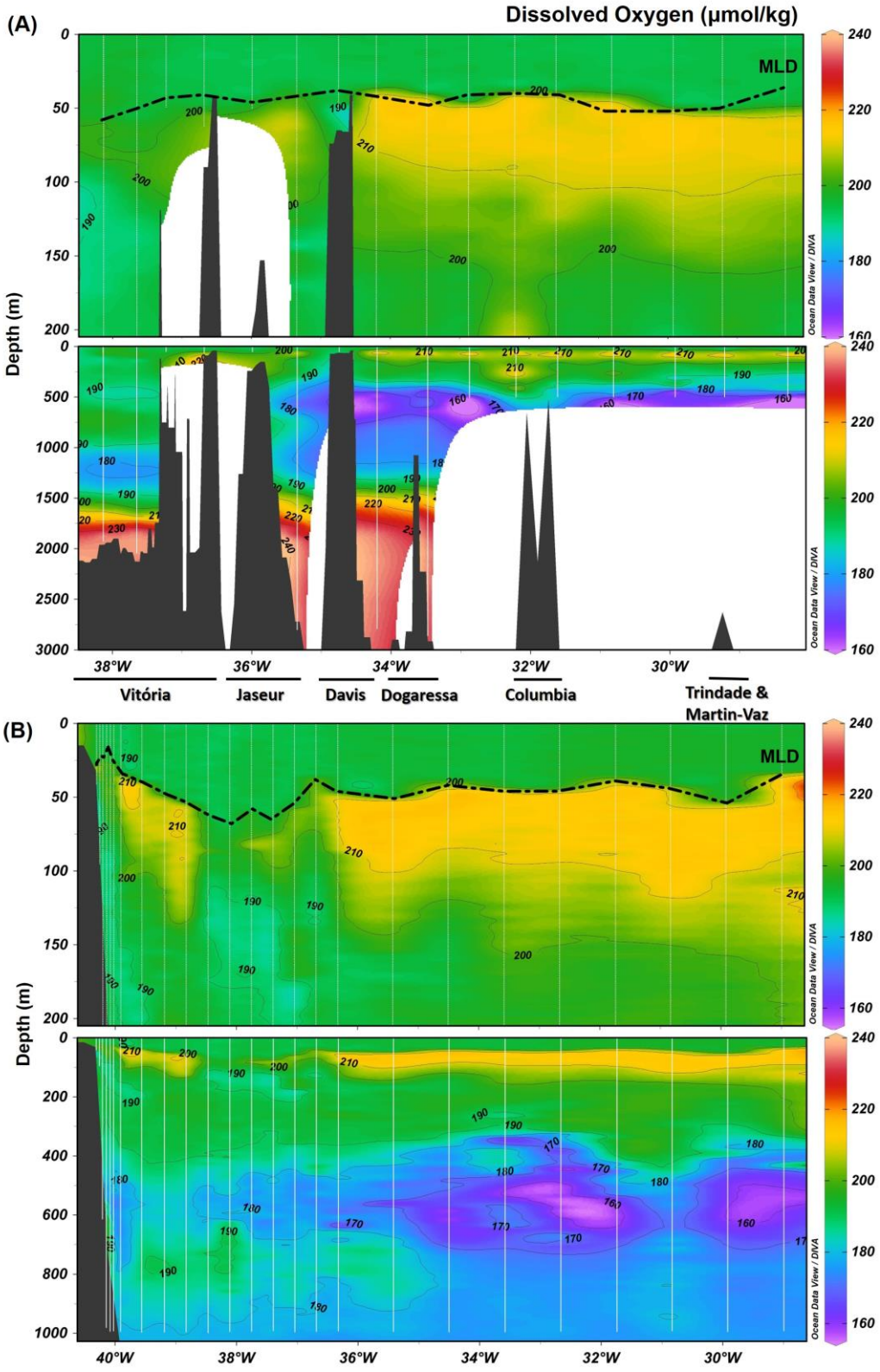

Figure 5: Distribution of dissolved oxygen (µmol/kg) for (A) section A; and (B) section B. The mixed layer depths *(*MLD*)* are indicated as a black dashed line. The VTC main topographic features names are indicated at the bottom of figure section A. White lines indicate station location.

Figure 6 presents the results from the eOMP analysis. Plots consist of distribution of water masses expressed as percentages. For the TW, the figure displays only the first 300 m of the water column for better visualization. The results from AABW are not shown because its contribution to the domain was minimal (less than 8%).

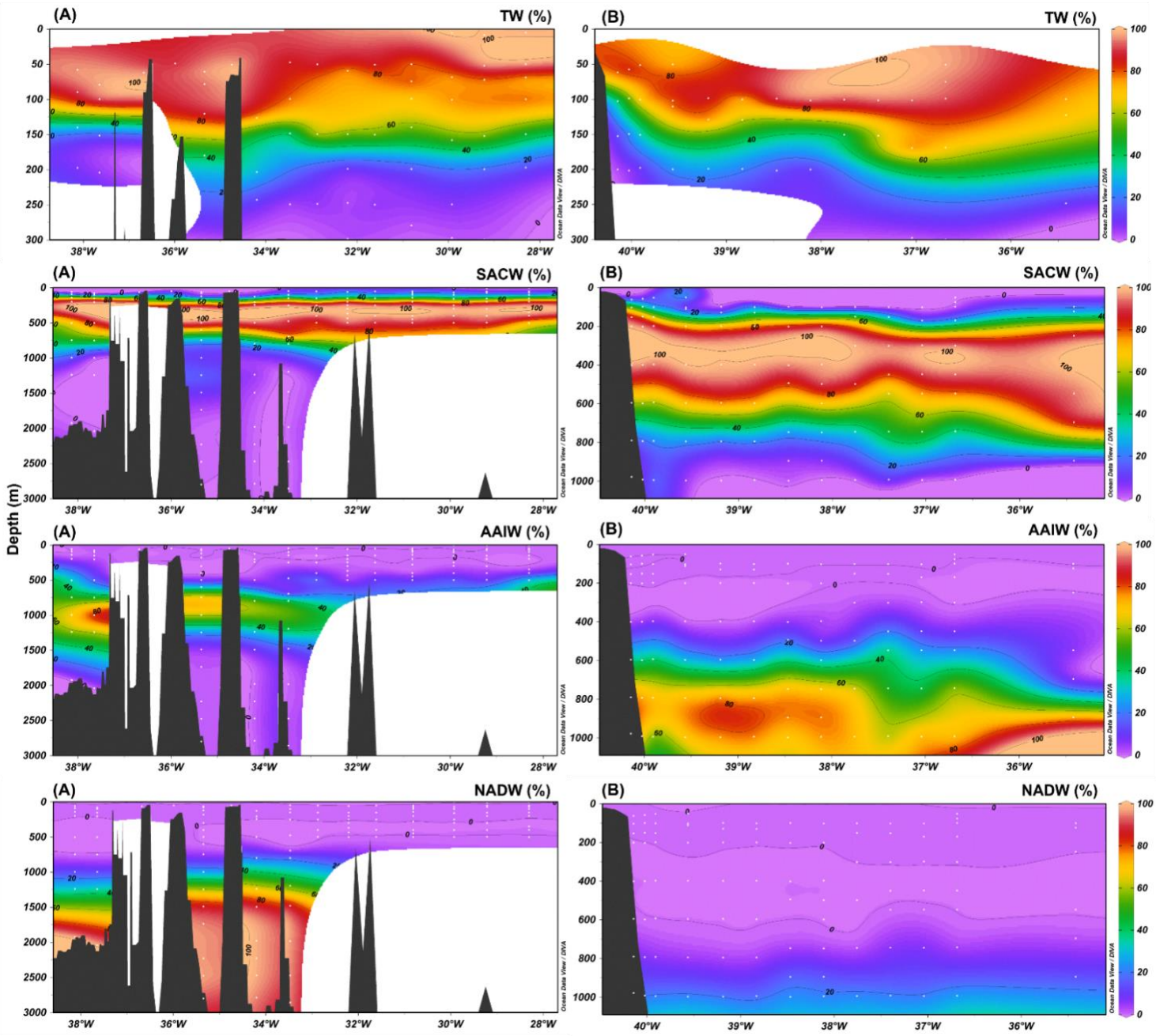

Figure 6: Distribution of water masses (%) for (A) section A; and (B) section B. TW: Tropical Water; SACW: South Atlantic Central Water, here is a sum of

$SACW_{upper}$ and $SACW_{lower}$; AAIW: Antarctic Intermediate Water; NADW: North Atlantic Deep Water, a sum of $NADW_{upper}$ and $NADW_{lower}$.

The MLD ranged from a minimum of 16 m on the shelf break and a maximum of 68 m at around 38° W in the B section. Most stations presented MLD of 40 – 50 m. The presented results were very similar to the ones found by Signorini et al. (1989). This stratified pattern is typical for the summer, as a result of a positive net heat flux (Ghisolfi et al., 2015). The observed MLD is completely homogeneous throughout both sections, suggesting the presence of a wind and wave driven MLD.

The potential temperature and salinity sections present the classical distribution of these properties for the tropical open ocean, in which greater temperatures and salinities (27°C and 37, respectively) were observed in the first meters of the water column. Also, a sharp thermocline/halocline was present between the MLD and 800m, separating the upper layer from the deep ocean. The ocean surface of the SAO is covered by TW as the mixed layer. It is a warm water mass with high salinity and is formed by the relatively high rates of evaporation in comparison to precipitation of the tropical Atlantic, carried towards the American coast by the SEC (Stramma and England, 1999). In the VTC region, the TW core (proportion of the water mass greater than 50%) occupied the first 150 m of the water column, which is consistent with the results from Álvarez et al. (2014).

The main feature of the sections is the presence of a nucleus with the highest temperatures and salinities observed within the surface, close to the continental slope at the region around 38° W, and corresponding to the maximum depth of the TW's 80% contour in section A. This feature is most likely due to the passage of the BC carrying TW southwards from its site of origin, flowing close to the continental slope. Evans et al. (1983) mentioned that the BC in the region of the VTC flows through the inshoremost region between the seamounts, but it can bifurcate or trifurcate along these western channels, reorganizing itself as a narrow current somewhere between 20°S and 21°S. The

values obtained by Evans and Signorini (1985) for the transport (corresponding to the 500 db level) in this region were approximately 4 Sv.

The VTC also marks the latitude of bifurcation of the westward SACW flow (Stramma and England,1999). Thus, north of the VTC, SACW flows northwards in opposite direction of the BC's flow, while south of it, SACW is incorporated to the BC, increasing its transport. The BC is present in both sections but better developed in section B, where a baroclinic signal is observed on the isotherms, which is accompanied with the deepest MLD observed. According to the analysis of isotherms in the region, Signorini et al. (1989) reported a disorganised current in the VTC region, while south of the VTC, the BC is better organised with clearer baroclinic signals, and the inclination of the isotherms shows an intensification of the geostrophic velocity. This is most likely due to the increase in the BC's transport and depth south of the VTC via contribution of SACW. Considering that, between its site of origin and the VTC, BC only carries TW, the BC's depth in the VTC region (section A) is approximately 150 m. However, south of the VTC, the SACW also flows southwards adding to the BC's transport. For this reason, it would be plausible to assume that in section B the BC's depths and transports would show greater values than in section A.

The core of SACW was found within the thermocline and centred at 500 m, occupying the water column between 150 and 650 m. It is a water mass with rather uniform properties throughout its range, characterised by a narrow straight line between the TS points (figure 2). De Souza et al. (2018) investigated the varieties of subtropical mode waters that compose SACW in the SAO, sourced (1) in the Brazil-Malvinas Confluence region; (2) in the Agulhas retroflection and Benguela Current region; and (3) in the southern edge of the subtropical gyre (Sato and Polito, 2014). The results suggest that the main varieties that compose the VTC region were the (2) at the upper levels of the thermocline (around the depths of 100 and 200 m), and the (3) at deeper levels (around the depths of 400 and 500 m). The results also demonstrated

that the variety sourced in the Brazil-Malvinas confluence (1) contributes less to this region, as it is regionally confined by the Brazil Current recirculation gyre.

Along its course in the subtropical gyre, the SACW also receives an input of thermocline and intermediate waters from the Indian Ocean (mainly Indian Central Water- ICW) through the leakage of the Agulhas Current Retroflection to the SAO (Gordon et al., 1992). However, the contribution of ICW was not evaluated in our study. According to Provost et al. (1999), this contribution of ICW in the SAO represents a small volume of water and with highly variable properties. In their analysis, Poole and Tomczak (1999) showed a very stratified SACW-ICW, with the SACW occupying the upper level of the thermocline layer, whilst ICW is carried by SEC across the SAO predominantly below 400 m. In its bifurcation, SEC turns into NBC -that feeds the northern hemisphere- and the BC -that feeds the subtropical gyre. However, due to the shallowness and weakness of the BC in its origin, ICW contributes little to the subtropical gyre, but is rather transferred equatorwards with the NBC.

The dissolved oxygen distribution is marked by a relative oxygen minimum layer (OML) between the depths of 400 and 800 m, which its minimum of ~160 µmol/kg is centred in the depth of 500 m, within the core of SACW. This oxygen minimum is a feature of the lower SACW in tropics, which indicated the low rates of renewal in this region (Stramma and Schot, 1999). Accordingly, this oxygen minimum is not a continuous layer but sometimes even consists of two minima. In addition, this depth is often associated with an accumulation of organic sinking particles, resulting in high rates of remineralisation of organic matter and, consequently, a high demand for dissolved oxygen (Libes, 2009).

The AAIW present in the SAO is formed north of the Sub-Antarctic Front and east of the Drake Passage. It is characterised by a salinity minimum and a slightly shallower dissolved oxygen maximum. It is carried northwards to the SAO in the western boundary (Piola and Gordon, 1989) and around the subtropical gyre, when then it returns to the American coast and bifurcates at around 28°S (Boebel et al., 1999). South of this latitude, AAIW is incorporated

to the BC's flow; and north of it, it flows northwards with the IWBC through the VTC (Soutelino et al., 2013).

The distribution of AAIW in the VTC region was centred at 900-1000 m and was marked by a core of higher concentrations (80%) at around 38°W, where it was found the lowest salinity (about 34.35) in the sections. In addition, the low salinity core (salinities equal/lower than 34.4) associated with the AAIW is considerably thicker (400 m, extending from 650 to 1050 m) around 38°W than the offshoremost stations (70 m, extending from 765 to 835 m). This feature is most likely associated to the passage of the IWBC. According to Talley (1996), in the tropics the salinity is indeed lower in the location of the western boundary current.

The oxygen maximum, a striking characteristic of the AAIW, is only present on the region of the passage of the IWBC, and not observed offshore of it (figure 7). This indicates that the AAIW carried by the IWBC through the inshoremost channel between the seamounts is somewhat more recently ventilated and less diluted than the surrounding intermediate waters. Several authors (e. g. Talley, 1996; Warner and Weiss, 1992) have reported that the AAIW dissolved oxygen maximum extends northwards to the equator as a tongue in the IWBC region, despite having its northern limb on the subtropical/subequatorial front at 20-21°S in the open ocean (Tsuchuya et al., 1994). The termination of the AAIW oxygen maximum north of 21°S is related to the circulation. The AAIW south of 21°S is newer and circulating anticyclonically in the subtropical gyre. The AAIW with lower dissolved oxygen north of 21°S is the southern westward-flowing limb of the cyclonic subequatorial gyre, in which the AAIW was advected eastward near the equator and is returning westward farther south. In this gyre, the AAIW oxygen is severely reduced by consumption (Tsuchuya et al., 1994).

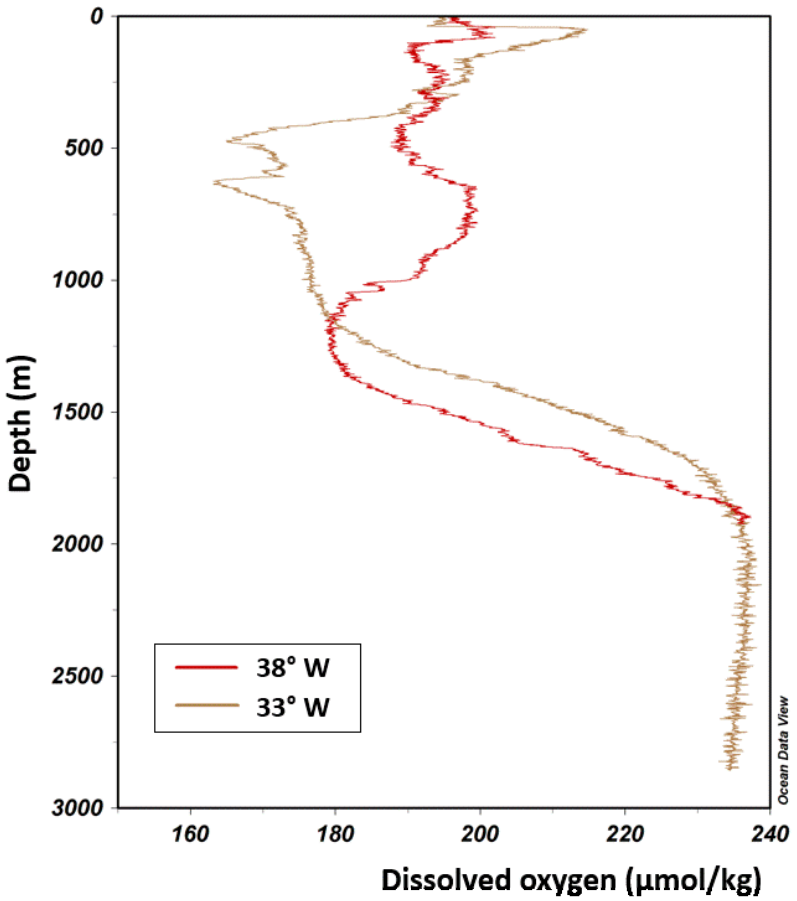

Figure 7: Dissolved oxygen (µmol/kg) profile for the station located at 38° W (red line) and the station located at 33°W (brown line).

Consequently, the dissolved oxygen distribution is profoundly affected by the distribution of the water masses, as indicated in figure 7. At 38° W, in the longitude of the passage of the western boundary current system, the AAIW's oxygen maximum (199 µmol/kg) is observed between the depths of 650 and 850 m. This is followed above by a less developed SACW's OML at 500 m. In contrast, at 33° W, the AAIW dissolved oxygen maximum is not observed, but a further developed SACW's two dissolved oxygen minima (of about 160 µmol/kg) can be seen at the depths of 475 and 630 m.

Although the UCDW has not been included in our analysis, data showed evidence of its occurrence in the narrow region of the western boundary current system. Higher concentrations of inorganic macronutrients (discussed in the

next topic) were observed, especially silicate (around 35 µmol/kg), at slightly greater depths than the AAIW (around 1200 m), as seen in figure 9. This was associated with lower dissolved oxygen concentrations than offshoremost stations (figure 7). The UCDW is characterised by its low dissolved oxygen content and high concentration of inorganic macronutrients (Stramma and England, 1999). This occurs because this water mass is not formed in contact with the atmosphere by ventilation, but by the mixing of waters entering the Antarctic from mid-depths in the Indian, Pacific and Atlantic with Weddell Sea Bottom Water and deep water from the North Atlantic (Broecker et al., 1985). These higher/lower concentrations of inorganic macronutrients/dissolved oxygen, characteristic of the UCDW, are not observed in the other offshore stations. Hence, it provides evidence that the UCDW may have a stronger contribution reaching at least as north as 20°S in the region close to the continental slope, carried by the IWBC; while for the offshore stations, the contribution is probably minimal, as AAIW is the dominant water mass in UCDW maximum as proposed by Álvarez et al. (2014).

The NADW is formed in the northern hemisphere and is carried to the SAO by a narrow DWBC that flows southwards transporting 14 Sv, close to the continental slope, in the opposite direction of the IWBC (Garzoli et al., 2015). South of 8°S, the DWBC breaks into rings, becoming a non-steady current (Dengler et al., 2004). By the time the DWBC reaches the VTC, the flow follows two different pathways. The main portion of the NADW flow continues along the continental shelf of South America, while a smaller portion flows towards the interior of the SAO (Garzoli et al., 2015).

The NADW is characterised by higher salinity and dissolved oxygen concentrations than the surrounding water masses (Vanicek and Sieldler, 2002). In our study, the NADW core appeared to cover a thick layer, extending from about 1200 m to the deepest depth sampled (3000 m). This result is consistent with Herrford et al. (2017), who found NADW occupying the depths between 1200 and 4000 m in the tropical SAO. The distribution of NADW close to the continental slope is slightly deeper (1500 m) than in the offshore stations.

This feature can be explained by the thicker and greater contribution of AAIW in the region, and by the possible contribution of UCDW. The latter assumption is supported by the observed deeper dissolved oxygen maximum of the NADW at 38°W (figure 7), which was likely influenced by the oxygen minimum of UCDW from above.

De Carvalho-Ferreira and Kerr (2018) results indicate that the main contributor to the NADW in the studied region (down to 3000 m) is the Labrador Sea Water, which increases its contribution between the equatorial region and the subtropical region from 40% to 70%. According to the authors, this enrichment suggests a deepening of the Labrador Sea Water core, as a response to the presence of subtropical gyre. Hence, the Labrador Sea Water core is found shallower than 2000 m north of 30°S. These findings agree with our results, which showed an upperNADW (which comprises the Labrador Sea Water and the Mediterranean Water) covering a layer shallower than 2000 m (between 1200 and 2000 m), while lowerNADW covered between 2000 and 3000 m in the water column.

The distribution of dissolved oxygen and salinity (which are the main indicators of this water mass) in the core of NADW were uniformly distributed. As mentioned by Demidov (2003), the distinction between the different components of NADW are not clear south of 20°S, as a strong similarity between them can be observed. This is because upon arrival in the Brazil Basin, the NADW characteristics are the result of strong modifications that occurred throughout its passage from the site of origin into the tropical SAO (Herrford et al, 2017).

3.2. On the dynamics of chlorophyll and inorganic macronutrients of the Vitória-Trindade Chain region

The distribution of chlorophyll for sections A and B are presented in figure 8 in the same format of the potential temperature, salinity and dissolved oxygen figures, but only the first 200 m of the water column are shown for better

visual presentation. In the following paragraphs, the distribution of chlorophyll will be discussed in relation to the distribution of dissolved oxygen (figure 5) presented in the previous section. It is worth pointing out that in situ chlorophyll fluorescence is proxy for chlorophyll concentration (hence phytoplankton biomass), but there are still large natural variations in the relationship between in situ fluorescence and extracted chlorophyll concentration (Roesler et al., 2017). Despite that, our chlorophyll concentrations were found in agreement with the values reported by de Souza et al. (2013) for the Fernando de Noronha and São Pedro e São Paulo islands region, located in tropical South Atlantic Ocean. The summer chlorophyll concentrations from the VTC region ranged from 0.18 to 2.44 µg/L, while the reported values from summer and autumn ranged from 0.08 to 3.91 µg/L (de Souza et al., 2013).

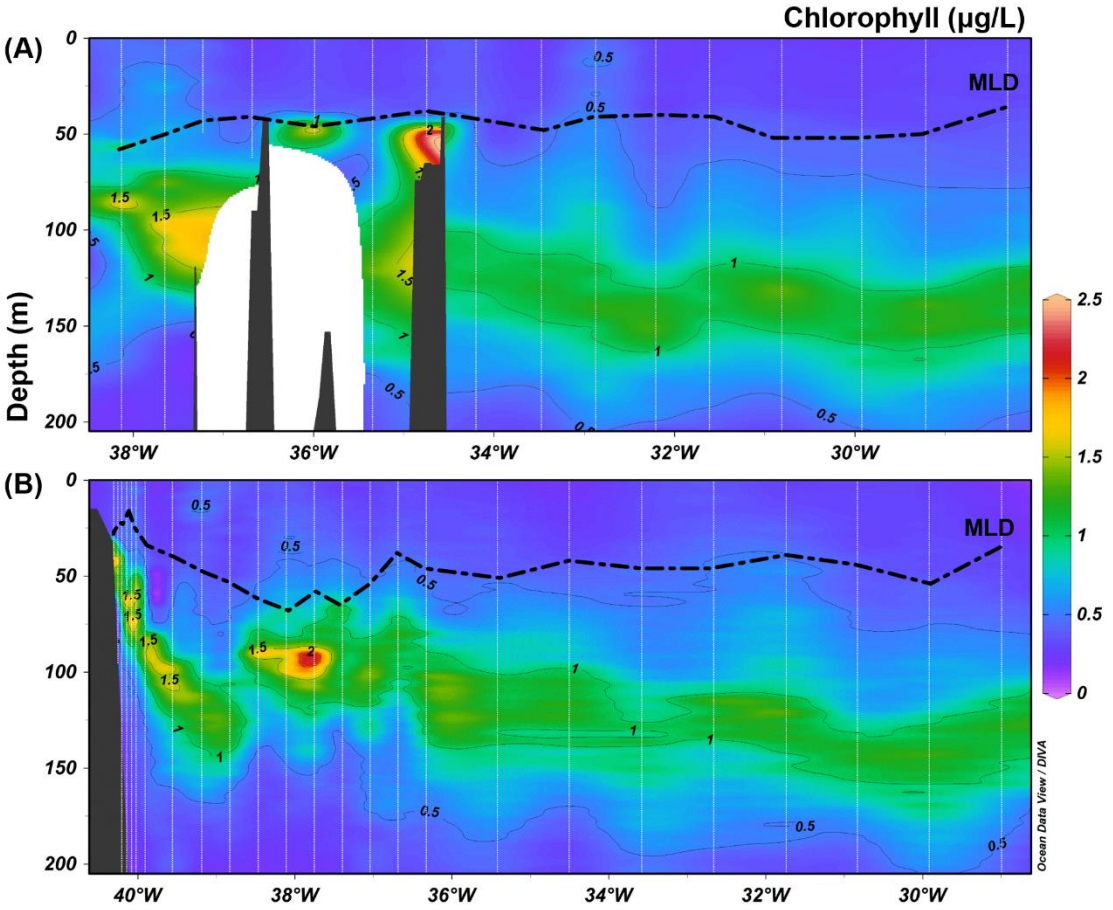

Figure 8: Distribution of chlorophyll (µg/L) for the first 200 m of the water column for (A) section A; (B) section B. The MLDs are indicated as a black dashed line.

For the names of the VTC main topographic features, see Fig. 3 (A). White lines indicate station location.

The dissolved oxygen distribution is marked by a strong oxygen maximum (210 µmol/kg) layer between a depth of 50 and 100 m (figure 5), which is well distributed immediately below the MLD. Below the oxygen maximum depth, centred at about 100 m, we also find the chlorophyll maximum at the subsurface (figure 8). Here, maximum values (approximately 2 µg/L) were found close to the continental slope, where the BC flows through the seamounts, as well as in summits of the Jaseur and Davis seamounts. Subsurface chlorophyll maxima are a common feature of tropical and subtropical oceans (Cullen, 1982; Huisman et al., 2006). According to Perry et al. (2008), the subsurface chlorophyll maximum may be due to the strong stratification observed in summer, which prevents the replenishment of nutrients from below. Lacking in nutrients, the productivity is limited on the surface, allowing light to penetrate deeper in the water column. Below the MLD, the nutrient concentrations are higher, allowing phytoplankton growth. Indeed, in the region of the VTC the deep chlorophyll maxima were found below the MLD, and the surface concentration of chlorophyll were very low (~ 0.3 µg/L). In spite of the relatively high concentration of chlorophyll found in the subsurface, Anderson (1969) pointed out that it might not represent a corresponding increase in phytoplankton volume, since it could be related to an adaptation of the cells to low light by an increase in their chlorophyll content. Despite that, these deep chlorophyll maxima still stand for significant rates of primary production (Anderson, 1969) and phytoplankton biomass (Furuya, 1990).

Intriguingly, the observed maximum in the dissolved oxygen concentration is not at the same depth as the subsurface chlorophyll peak as expected, but at slightly shallower depth. A similar pattern is found in summertime for oceanic waters at mid-latitude in the Pacific Ocean (Shulemberger and Reid, 1981). The presence of this pattern had been related to the summer loss of oxygen above the MLD owing to the warming of the upper waters (Pytkowicz 1964), which could explain its distribution immediately

above the MLD. However, Anderson (1969) argued that the summer loss of oxygen could not explain its total increment and suggested that it was formed largely by photosynthetic production, especially in areas where the chlorophyll maxima were present. Shulemberger and Reid (1981) further added that the supersaturated oxygen maxima would accumulate just below the MLD because of the density barrier, which would prevent its equilibration with the atmosphere.

Lemos et al. (2018) found that the region of the VTC underwent seasonal blooming, mostly in the region of the Vitória bank and Jaseur seamount, with the peak of chlorophyll-a occurring around the austral winter. It was concluded that this seasonal blooming was controlled by the relation of the MLD and the depth of the seamounts' summits. In the winter, there are stronger winds and waves in the region (Pianca et al., 2010), leading to deeper MLD than the summits of the seamounts, thus enhancing vertical mixing and fertilizing the upper ocean. The results found by Sonnekus et al. (2017) support this hypothesis, as a positive contribution to the phytoplankton biomass was found in the Melville bank in the Southern Indian Ocean. However, our observed summer MLD was shallower than the summits of the seamounts, which explains the absence of the surface chlorophyll bloom associated with the seamounts in this season.

Although we found relative shallow MLD along the sections, for the stations close to the shelf break at around 38° W, in section B, there is a deepening of the MLD. This may explain the increased chlorophyll concentration (approximately 2,3 µg/L), as a deepening of the MLD could enhance nutrient levels in the euphotic zone. In addition, the deepening of the MLD could have eroded the oxygen subsurface maxima trapped below the density barrier, allowing for equilibrium with the atmosphere. This would explain the observed discontinuation of the subsurface oxygen maxima in the region of the deepest MLD.

There is also a peak of chlorophyll (approximately 2,3 µg/L) on the summit of the Davis seamount, which may be attributed to the formation of a Taylor Cap (Proudman, 1916; Taylor, 1917). The theorem requires that in a

rotating environment in geostrophic balance, the flow of a homogeneous fluid cannot cross isobaths. Therefore, upon encountering a seamount, the flow must move around the topography rather than over it. This may create both an anticyclonic flow and isopycnal lifting over the seamount, generating a region of trapped fluid (Chapman and Haidvogel, 1992; Clark et al., 2010). The residual circulation may cause the retention of organic/inorganic matter; and the uplifting of isopycnals may bring nutrient rich water to the seamounts' summit. This in turn increases primary production, especially when shallow summits penetrate the euphotic zone (Dower et al., 1992; Genin and Boehlert, 1985).

Since the VTC is a perpendicular topographical barrier to the passage of the BC, the region is favourable to the generation of a Taylor Cap. This could explain the higher chlorophyll concentrations on the seamounts' summits. Genin and Boehlert (1985) had observed the uplifting of isotherms in the form of a Taylor Cap on a seamount in the Pacific Ocean, which was associated to high chlorophyll concentrations on the summit. In the study conducted by de Souza et al. (2013) in the São Pedro e São Paulo archipelago and in the Fernando de Noronha Chain located in the tropical south-western Atlantic, the researchers observed an upward entrainment of cold and nutrient-rich water in the region of the seamounts, which could be an evidence of the formation of a Taylor Cap. Nevertheless, despite the observance of higher chlorophyll concentrations in the seamounts' summits, which is a feature of a Taylor Cap, such isopycnal lift is not observed in our data.

The enhancement of chlorophyll concentrations on the seamounts' summits could also be related to a benthic-pelagic coupling effect as proposed by Meirelles et al. (2015). The authors observed a high correlation between the VTC's rhodolith beds microbial abundance, richness and diversity and the chlorophyll concentrations, even though there was no local upwelling. The proposition was that exudates and excreted organic and inorganic nutrients by benthic organisms could help microbes grow in the surrounding waters. This was supported by the presence of high concentrations of dissolved organic carbon (DOM) in all the seamounts' summits.

Moreover, the presence of reef systems generates habitat complexity, which enhances herbivory and increases fish density and biomass (Graham and Nash, 2013). Consequently, the region might constitute a hotspot for foraging migrators (Reid et al., 1991; McManus et al., 2008), which contribute to the dissolved and particulate organic matter (POM) through defecation and messy feeding in the seamount region (Djurhuus et al., 2017). Once POM and DOM are released and there is a high abundance of microbes, the organic matter is rapidly recycled and taken up by the phytoplankton. The lower dissolved oxygen concentration (about 190 µmol/kg) found in the chlorophyll maxima in the Davis seamount summit supports this hypothesis.

Figure 9 presents the distributions of pH, phosphate, nitrate and silicate as measured from samples from the Niskin rosette for sections A and B. The range of the concentrations found was, generally, consistent with those reported by Mawji et al. (2015). The distribution of these parameters portrayed the typical vertical structure associated to biogenic matter production and remineralisation along the density gradient. Hence, the minimum inorganic macronutrient concentrations were found at the surface, and there is an enrichment within the thermocline, accompanied by the minimum oxygen layers.

An increment in the inorganic macronutrient concentrations is not observed at the surface at the seamounts, differing from previous reports for the region (Gaeta et al., 1999; Rezende et al., 2006; Braid, 2008), even though most of these were not for the summer period. Braid (2008) suggested that the high inorganic macronutrient concentrations found in the VTC were related to the deepening of the mixed layer, especially during the fall and winter, rather than in summer. Therefore, the low concentrations of inorganic macronutrients at the surface of the VTC may be related to the strong stratification of the water column observed in summer, which prevents replenishment of nutrients from below. This supports the observance of the highest concentrations of chlorophyll in a subsurface layer, below the MLD, where the concentrations of inorganic macronutrients were higher, since the phytoplankton growth is limited

by the light supplied from above and nutrients supplied from below (Huisman et al., 2006).

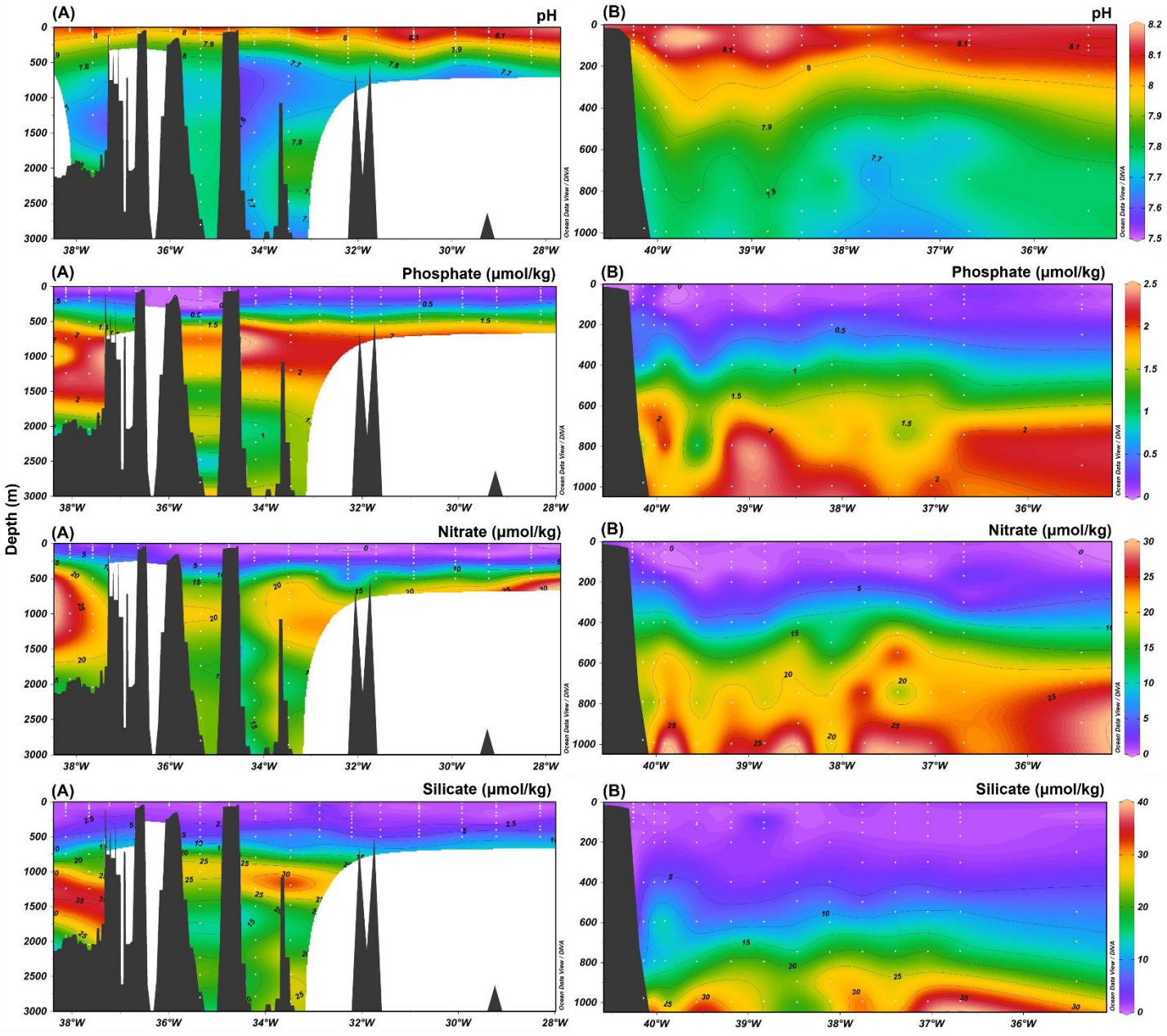

Figure 9: Distribution of pH and dissolved inorganic macronutrients (µg/L) for (A) section A; and (B) section B. For the names of the VTC main topographic features, see Fig. 3 (A). White dots indicate sample depth.

The distribution of pH (figure 9) was very similar to the distribution of dissolved oxygen (figure 5), which reflects the process of formation and destruction of organic matter. At the surface, we observe typical oceanic high pH values (8.15) since the uptake of carbon dioxide during photosynthesis leads to an increase in the pH of the water. Conditions of lower pH are caused by the aerobic oxidation of organic matter, which releases carbon dioxide and inorganic macronutrients and consumes dissolved oxygen (Libes, 2009). Therefore, the lower pH and dissolved oxygen and higher inorganic macronutrient concentrations observed in the central/intermediate layer may reflect strong remineralisation of organic matter, associated with a small advection process (Wyrtic, 1962) and older water masses. Differing from this general pattern, higher pH and lower concentrations of inorganic macronutrients were observed around 35°W between the Jaseur and Davis seamounts. This finding may be a response to the complex dynamics of the region. Prominent characteristics of the Brazilian western boundary current system are: the presence of intense mesoscale activity in the study region, exhibiting cyclonic and anticyclonic meanders (da Silveira et al., 2004; Fernandes et al., 2009); the presence of the Vitória Eddy (Schmid et al., 1995), which sometimes translates equatorward through the VTC (Arruda et al., 2013); and flow disturbance generating turbulence associated to topographic features (Lueck and Mudge, 1997; Heywood et al., 1990; Hasegawa et al., 2004).

The nitrate distribution was well correlated to phosphate (R^2 = 0.9) and presented a ratio of 11.4. This dissolved [N]/[P] concentration ratio is much lower than the classical 16:1 Redfieldian stoichiometry (Redfield et al., 1963). Despite that, our N/P ratio is within the range reported by Borges-Carvalho et al. (2018), in which a ratio of 15±3.6 (varying from 10.1 to 25.1) was found for the waters deeper than 100 m in the continental shelf and slope of the western SAO. Anderson and Sarmiento (1994) had found a lower $R_{N/P}$ remineralisation ratio in the 1000-3000 m zone of about 12±2, similar to the concentration ratios found here. According to the authors, this lower ratio is associated with sedimentary denitrification in this layer, which occurs in low oxygen conditions, converting nitrate to nitrogen gas.

The dissolved [N]/[P] concentration ratio depth plot (figure 10) resembles the “T shape” demonstrated by Fanning (1992) for the Atlantic Ocean. However, it is asymmetrical, presenting a considerably bigger right arm, reflecting bigger [N]/[P] ratios in the first 100 m of the water column. The most reasonable explanation for this result is the nitrogen fixation by *Oscillatoria* (*Trichodesmium*) spp., since its colonies utilise elemental atmospheric nitrogen, which is not part of the usual pool of dissolved inorganic macronutrients (Fanning et al., 1992). During the cruise, an extense *Trichodesmium* spot was identified on the surface of the continental slope region (figure 11).

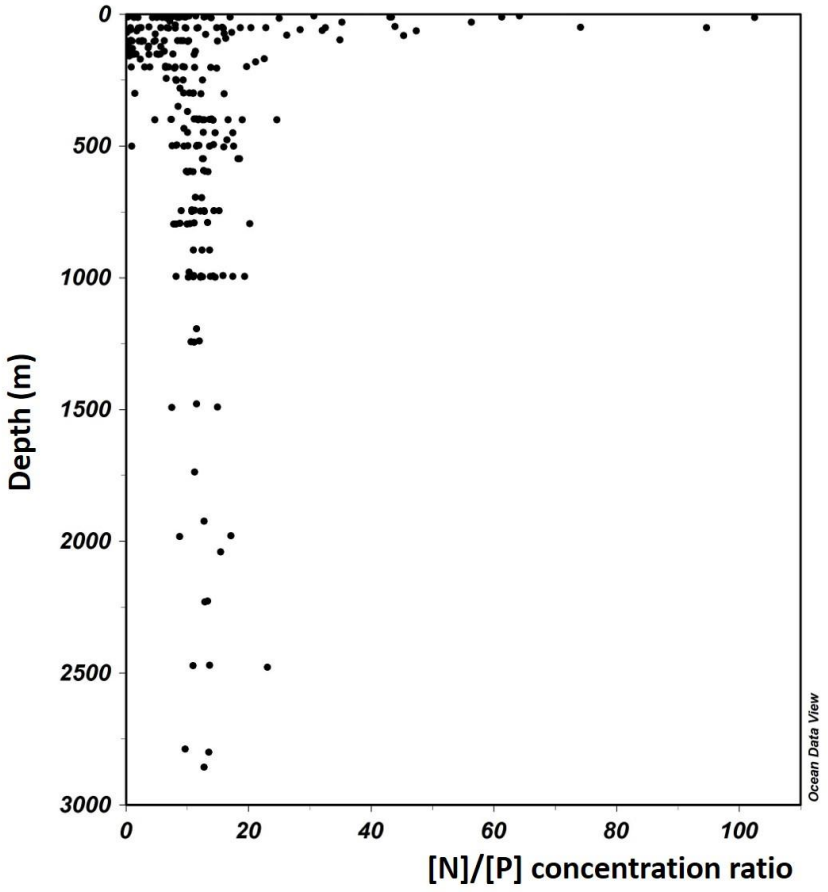

Figure 10: Profile of the dissolved nitrate and phosphate concentration ratios in the sampled depths.

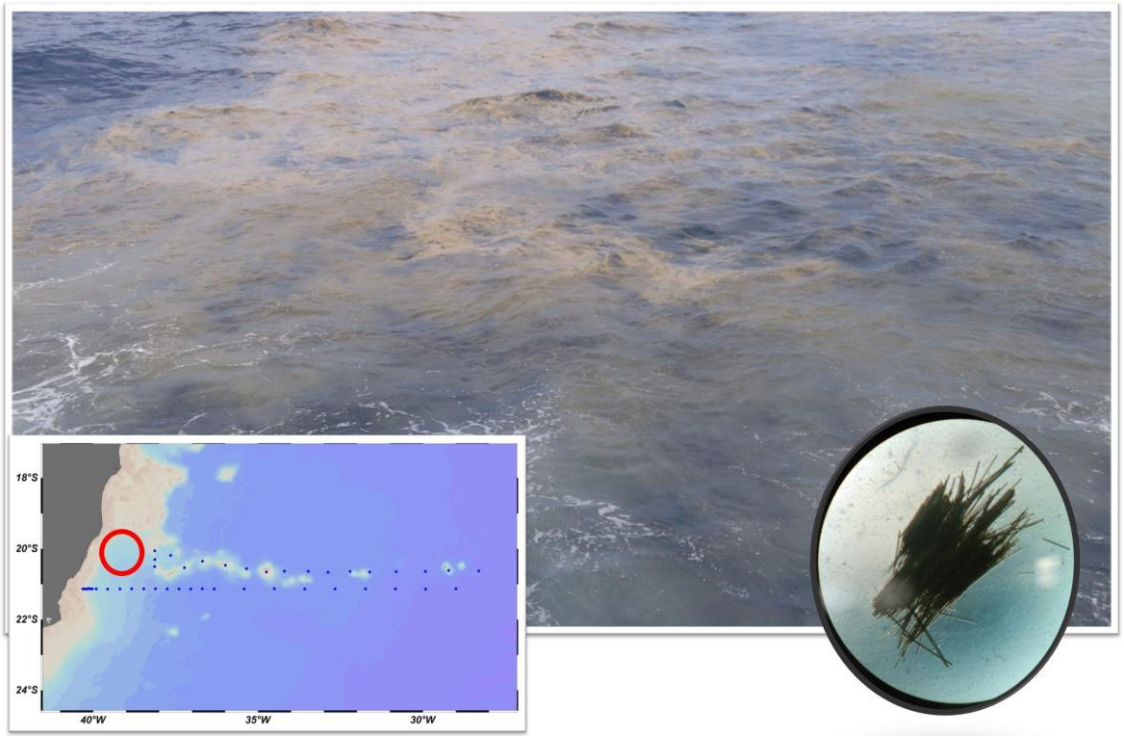

Figure 11: Location of the *Trichodesmium* spot observed in the region of the continental slope in section A (red circle).

However, the distribution of silicate was more poorly correlated to the phosphate (R^2 = 0.71), presenting a ratio of 10.15, which is very similar to the 10.3 regeneration ratio calculated by Poole and Tomczak (1999) for the thermocline waters of the SAO. The lower [Si]/[P] correlation is probably related to a shift of linearity, that separates the upper and deep ocean. For depths lower than 500 m, there were greater correlations (R^2 = 0.72) and a dissolved [Si]/[P] concentration ratio of 5.9. However, for depths greater than 500 m, a [Si]/[P] correlation was not detected (R^2 = 0.05), and its ratio was 76.

Table 3 presents the mean values of estimated remineralised nitrate and phosphate for SACW, AAIW and NADW, based on the AOU values. The higher the AOU, the greater the amount of dissolved oxygen removed since the last time the water mass was at the sea surface and greater the amount of remineralised nitrate and phosphate. Thus, AOU increases with increasing distance from the site of origin and the age of the water mass (Libes, 2009).

The amount of remineralised nitrate and phosphate calculated based on the ratios proposed by Guglielmi et al. (2017) was always greater than when based on the ratios of Anderson and Sarmiento (1994), by approximately 2 and 0.25 µmol/kg for nitrate and phosphate, respectively.

The greater occurrences of AOU and remineralised nitrate and phosphate were found primarily in the AAIW, and in the lower limb of SACW. This result reflects the much older and oxygen poor AAIW observed in the stations away from the continental slope. This is because this water, after being carried as an IWBC, travelled all the way across the equatorial region and, then, it returned to the VTC, having its dissolved oxygen content increasingly reduced along the way (Tsuchuya et al., 1994). The observance of lower AOU in the core of AAIW in the region of the IWBC (data not shown) reinforces these findings. Despite being a relatively old water mass (as it takes approximately 26 years to reach the equatorial region of the Atlantic Ocean, Andrié et al., 2002), NADW showed lower values of remineralised nitrate and phosphate than AAIW. This is related to the lower demand of dissolved oxygen and consequent remineralisation rate in these deep levels of the ocean, since the deposition rates of sinking particles decrease significantly with depth.

Table 3: Estimation of the mean amount and standard deviations of nitrate (N) and phosphate (P) (µmol/kg) remineralised in each water mass since leaving the surface. The calculation was made based on the remineralisation ratios proposed by Anderson and Sarmiento (1994) and Guglielmi et al. (2017).

	Anderson and Sarmiento (1994)		**Guglielmi et al. (2017)**	
	N	**P**	**N**	**P**
SACW	6.67±2.88	0.42±0.18	8.80±3.48	0.56±0.23
AAIW	12.52±0.90	0.78±0.06	14.62±1.05	1.01±0.07
NADW	9.15±1.22	0.57±0.08	11.43±	0.76±

4. Conclusions

In this study, eOMP analysis was successfully performed to determine the distribution and contribution of water masses along the VTC, located in the western South Atlantic Ocean. The VTC is located in the region of a subtropical/subequatorial front, although its water mass distribution displayed mainly subequatorial characteristics. However, the water masses presented a differentiation of its features in the inshoremost passage between the Vitória seamount and the continental shelf. This is related to the passage of the western boundary current system. In this region, a more recently ventilated and less diluted AAIW (as observed by the relatively high oxygen tongue) was observed.

In addition to determining the distribution of water masses, this paper aims to elucidate the configuration of hydrographic and chemical proprieties in the yet poorly sampled South Atlantic Ocean. The inorganic macronutrient concentrations were not higher above the seamounts than in other oceanic areas, as a result of the shallow summer stratification of the water column. Consequently, no surface bloom was seen associated to the seamounts, corroborating with the findings of Lemos et al. (2018). On the other hand, the primary productivity and biogeochemistry in the vicinity of the seamounts seem to be more complex than previously assumed and possibly affected by pelagic-benthic interactions. Despite not observing a surface bloom, we found a well-developed deep chlorophyll maximum, which presented concentrations that were twofold higher within the seamounts' summits. This suggests, as opposed to previous assumptions, that the VTC may still play an important role on the primary productivity during the austral summer.

Acknowledgements

The authors wish to acknowledge all the people who helped in field sampling and analyses. This article is a contribution to the "*Pode um arquipélago fertilizar o oceano? Um Estudo Multi-Disciplinar para a*

Investigação do "Efeito-Ilha" na Cadeia Vitória-Trindade" project (CNPq 458583 - 2013/8), which receives support from the Conselho Nacional de Desenvolvimento Científico e Tecnológico (CNPq). E. B. Rocha acknowledges the scholarship and financial support from the CNPq.

Capítulo IV:

Síntese de Resultados e Discussões

3. Síntese de resultados e discussões

A coluna de água da região da Cadeia Vitória-Trindade mostrou-se bem estratificada, com uma camada de mistura de, em média, 43±11 m, o que é característico para o período de verão no oceano tropical. Devido a esta rasa estratificação da coluna de água, as concentrações de macronutrientes inorgânicos dissolvidos na camada de mistura foram consideravelmente baixas, além de não terem sido observadas maiores concentrações associadas à região dos montes submarinos, diferente do reportado previamente para a região (Braid, 2008; Rezende et al., 2006; Gaeta et al., 1999). Este resultado é corroborado pelo proposto por Lemos et al. (2018), no qual os blooms fitoplanctônicos superficiais na região dos montes submarinos ocorreriam de forma sazonal, com pico nos meses de inverno, como resultado da sazonalidade da profundidade da camada de mistura. Ou seja, nos meses de inverno a camada de mistura é mais profunda que os cumes dos montes submarinos, o que facilitaria o fluxo de nutrientes para a camada mais superficial do oceano e, consequentemente, formaria os blooms superficiais.

Entretanto, nossos resultados demonstram que a dinâmica sazonal de produtividade na região dos montes submarinos pode ser mais complexa do que assumido anteriormente. Apesar de terem sido observadas baixas concentrações de clorofila nas camadas superficiais dos oceanos, observou-se um máximo de clorofila subsuperficial bem desenvolvido na profundidade de aproximadamente 100 m, o qual apresentou concentrações até duas vezes maiores na região dos cumes dos montes de Davis e Jaseur. Esse máximo de clorofila pode ser formado em camadas subsuperficiais quando a concentração de macronutrientes inorgânicos é baixa em superfície e a luz penetra até maiores profundidades na coluna de água, onde a concentração de macronutrientes inorgânicos é maior.

Por sua vez, as maiores concentrações de clorofila associadas ao cume dos montes submarinos podem estar relacionadas a fatores físicos como a formação de células de circulação que acumulam fitoplâncton, partículas e matéria orgânica/inorgânica, apesar de não ter sido observada nenhuma

elevação isopicnal associada aos montes submarinos. Outra explicação inclui interações entre o ambiente bêntico e pelágico, no qual as exsudações e excreções dos organismos bentônicos dos cumes dos montes estimulariam o crescimento de microrganismos, que reciclariam a matéria orgânica, aportando macronutrientes inorgânicos para os produtores primários. Além das excreções e exsudações dos organismos bentônicos, vale ressaltar que ambientes de montes submarinos são atrativos para herbívoros e predadores que migram para essas regiões, aportando matéria orgânica dissolvida e particulada para região através da alimentação e excreção.

Imediatamente abaixo da camada de mistura, foi observado um máximo subsuperficial de oxigênio dissolvido na profundidade de aproximadamente 60 m, intrigantemente mais raso que o máximo subsuperficial de clorofila. Essa distribuição pode estar associada a perda de oxigênio dissolvido acima da camada de mistura pelo aquecimento superficial de suas águas e diminuição da solubilidade dos gases. Tal hipótese explicaria o fato da distribuição do máximo de oxigênio dissolvido parecer “contornar” a linha de profundidade da camada de mistura. Outra possível explicação seria que este máximo de oxigênio dissolvido seria formado pela produção fitoplanctônica no máximo subsuperficial. Então, esta camada supersaturada de oxigênio dissolvido seria acumulada abaixo da camada de mistura, visto que a barreira de densidade não permitiria o seu equilíbrio com a atmosfera.

Os resultados também evidenciaram a passagem do sistema de correntes de contorno oeste através dos montes submarinos nas longitudes próximas de 38° W. Nas camadas mais superficiais, a passagem da Corrente do Brasil foi observada como um núcleo de águas mais quentes e salinas entre os montes de Vitória e Jaseur, os mais próximos da quebra de plataforma. Na seção B, a passagem da Corrente do Brasil também foi evidenciada por um aprofundamento das isotermas e da profundidade da camada de mistura, que atingiu 70 m neste ponto. Este aprofundamento da camada de mistura pela passagem da Corrente do Brasil foi responsável por um aumento nas concentrações de clorofila subsuperficiais nesta região, visto que promoveria

um aumento das concentrações de nutrientes acima da camada de mistura. Além disso, o aprofundamento da camada de mistura também foi responsável por “erodir” o máximo subsuperficial de oxigênio dissolvido, uma vez que é observada uma descontinuidade nesta região.

A Cadeia Vitória-Trindade está localizada na região de frente subtropical/subequatorial, que divide as regiões dos giros subtropical e equatorial. Entretanto, de forma geral as massas de água da região apresentaram características subequatoriais, nas quais são observadas características de massas de água mais antigas na porção central e intermediária (Água Central do Atlântico Sul e Água Intermediária Antártica, respectivamente), evidenciadas pelas menores concentrações de oxigênio dissolvido e maiores valores de utilização aparente de oxigênio. Isto ocorre, pois, estas massas de água são carregadas para norte pela corrente de contorno oeste, incluídas no giro equatorial e, após terem suas concentrações de oxigênio dissolvido bastante reduzidas, finalmente atingem a área de estudo.

Já no canal entre o monte de Vitória e o talude continental, região de passagem da Corrente Intermediária de Contorno Oeste, são observadas massas de água mais recentemente ventiladas, características do giro subtropical. Isto é evidenciado pela presença do máximo relativo de oxigênio característico da Água Intermediária Antártica e por seus menores valores de salinidade na região. Além disso, nesta região, a Água Profunda Circumpolar Superior parece ter alguma influência na profundidade de 1200 m, enquanto isto não é identificado para as estações localizadas na porção mais *offshore*.

Salienta-se que a as águas-tipo escolhidas para representar a distribuição da Água Central do Atlântico Sul (retiradas de Poole & Tomczak, 1999) na área de estudo devem ser melhor investigadas, visto que a variedade de maior densidade (lowerSACW) encontra-se muito próxima ao domínio da Água Intermediária Antártica. Isto pode ter resultado as baixas concentrações de Água Intermediária Antártica encontradas, e uma distribuição de Água

Central do Atlântico Sul atingindo até altas profundidades na coluna de água (e.g. 30% de contribuição em 800 m de profundidade).

As concentrações de nitrato e fosfato apresentaram alta correlação e uma razão de 11,4, a qual é consideravelmente inferior à proposta por Redfield. Nas camadas mais superficiais da coluna d'água, essas razões foram bem elevadas (até 100), o que é possivelmente resultado do grande bloom de *Trichodesmium* observado nas estações próximas ao talude continental. As razões de silicato e fosfato, por sua vez, apresentaram menores correlações, resultado de uma mudança na linearidade separando a camada superior (profundidade menor que 500 m, de razão 5,9) e profunda do oceano (profundidade maior que 500m, de razão 76). A quantidade de nitrato e fosfato remineralizada foi calculada para cada massa de água, sendo que os maiores valores foram encontrados para a porção da Água Intermediária Antártica e para a porção inferior da Água Central do Atlântico Sul. Isto é resultado destas massas de água serem relativamente antigas, de baixa renovação na região, e serem encontradas em uma profundidade onde a remineralização de matéria orgânica ainda é intensa.

Referências Bibliográficas

Álvarez, M., Brea, S., Mercier, H., & Álvarez-Salgado, X. A. (2014). Mineralization of biogenic materials in the water masses of the South Atlantic Ocean. I: Assessment and results of an optimum multiparameter analysis. *Progress in Oceanography*, *123*, 1-23.

Alves, R. J. V. (1998). Ilha da Trindade & Arquipélago Martin Vaz: Um Ensaio Geobotânico. *Serviço de Documentação da Marinha*, Rio de Janeiro, 144 p.

Amado-Filho, G. M., Maneveldt, G., Manso, R. C. C., Marins-Rosa, B. V., Pacheco, M. R., & Guimarães, S. M. P. B. (2007). Estructura de los mantos de rodolitos de 4 a 55 metros de profundidad en la costa sur del estado de Espírito Santo, Brasil. *Ciencias marinas*, *33*(4), 399-410.

Anderson, G. C. (1969). Subsurface chlorophyll maximum in the northeast Pacific Ocean. *Limnology and Oceanography*, *14*(3), 386-391.

Anderson, L. A., & Sarmiento, J. L. (1994). Redfield ratios of remineralization determined by nutrient data analysis. *Global biogeochemical cycles*, *8*(1), 65-80.

Andrade, L., Gonzalez, A. M., Valentin, J. L., & Paranhos, R. (2004). Bacterial abundance and production in the southwest Atlantic Ocean. *Hydrobiologia*, *511*(1-3), 103-111.

Andrié, C., Rhein, M., Freudenthal, S., & Plähn, O. (2002). CFC time series in the deep water masses of the western tropical Atlantic, 1990–1999. *Deep Sea Research Part I: Oceanographic Research Papers*, *49*(2), 281-304.

Arístegui, J., Sangrá, P., Hernández-León, S., Cantón, M., Hernández-Guerra, A., & Kerling, J. L. (1994). Island-induced eddies in the Canary Islands. *Deep Sea Research Part I: Oceanographic Research Papers*, *41*(10), 1509-1525.

Arruda, W. Z., Campos, E. J., Zharkov, V., Soutelino, R. G., & da Silveira, I. C. (2013). Events of equatorward translation of the Vitoria Eddy. *Continental Shelf Research*, *70*, 61-73.

Boebel, O., Davis, R. E., Ollitrault, M., Peterson, R. G., Richardson, P. L., Schmid, C., & Zenk, W. (1999). The intermediate depth circulation of the western South Atlantic. *Geophysical Research Letters*, *26*(21), 3329-3332.

Brea, S., Álvarez-Salgado, X. A., Álvarez, M., Pérez, F. F., Mémery, L., Mercier, H., & Messias, M. J. (2004). Nutrient mineralization rates and ratios in the eastern South Atlantic. *Journal of Geophysical Research: Oceans*, *109*(C5).

Broecker, W. S., Takahashi, T., & Takahashi, T. (1985). Sources and flow patterns of deep-ocean waters as deduced from potential temperature, salinity, and initial phosphate concentration. *Journal of Geophysical Research: Oceans*, *90*(C4), 6925-6939.

Castello, J. P & Krug, L. C. (2015). *Introdução às ciências do mar*. Editora Textos, Pelotas, 601 p.

Chapman, D. C., & Haidvogel, D. B. (1992). Formation of Taylor caps over a tall isolated seamount in a stratified ocean. *Geophysical & Astrophysical Fluid Dynamics*, *64*(1-4), 31-65.

Christian, G. D. (2004). *Analytical chemistry*. John Wiley & Sons, United States of America, 848 p.

Clark, M. R., Rowden, A. A., Schlacher, T., Williams, A., Consalvey, M., Stocks, K. I., ... & Hall-Spencer, J. M. (2010). The ecology of seamounts: structure, function, and human impacts. *Annual Review of Marine Science*, *2*, 253-278.

Cullen, J. J. (1982). The deep chlorophyll maximum: comparing vertical profiles of chlorophyll-a. *Canadian Journal of Fisheries and Aquatic Sciences*, *39*(5), 791-803.

da Silveira, I. C. A., Calado, L., Castro, B. M., Cirano, M., Lima, J. A. M., & Mascarenhas, A. D. S. (2004). On the baroclinic structure of the Brazil Current–Intermediate Western Boundary Current system at 22–23 S. *Geophysical research letters*, *31*(14).

da Silveira, I. C. A., Schmidt, A. C. K., Campos, E. J. D., de Godoi, S. S., & Ikeda, Y. (2000). A corrente do Brasil ao largo da costa leste brasileira. *Rev. Bras. Ocean*, *48*(2), 171-183.

Dandonneau, Y. & Charpy, L. (1985). An empirical approach to the island mass effect in the south tropical Pacific based on sea surface chlorophyll concentrations. *Deep-Sea Research*, 32(6), 707-721.

de Almeida, F. F. M. (2007). Ilhas oceânicas brasileiras e suas relações com a tectônica atlântica. *Terrae Didatica*, *2*(1), 3-18.

de Carvalho Ferreira, M. L., & Kerr, R. (2017). Source water distribution and quantification of North Atlantic deep water and Antarctic bottom water in the Atlantic Ocean. *Progress in Oceanography*, *153*, 66-83.

de Souza, A. G. Q., Kerr, R., & de Azevedo, J. L. L. (2018). On the influence of subtropical mode water on the South Atlantic Ocean. *Journal of Marine Systems*, *185*, 13-24.

de Souza, C. S., da Luz, J. A. G., Macedo, S., Montes, M. D. J. F., & Mafalda, P. (2013). Chlorophyll a and nutrient distribution around seamounts and islands of the tropical south-western Atlantic. *Marine and Freshwater Research*, *64*(2), 168-184.

Demidov, A. N. (2003). Distinguishing the intermediate and deep water masses in the South Atlantic. *OCEANOLOGY C/C OF OKEANOLOGIIA*, *43*(2), 153-163.

Dengler, M., Schott, F. A., Eden, C., Brandt, P., Fischer, J., & Zantopp, R. J. (2004). Break-up of the Atlantic deep western boundary current into eddies at 8 S. *Nature*, *432*(7020), 1018.

Djurhuus, A., Read, J. F., & Rogers, A. D. (2017). The spatial distribution of particulate organic carbon and microorganisms on seamounts of the South West Indian Ridge. *Deep Sea Research Part II: Topical Studies in Oceanography*, *136*, 73-84.

Doty, M. S. & Oguri, M. (1956). The island mass effect. *Journal du Conseil*, 22 (1), 33-37.

Dower, J., Freeland, H., & Juniper, K. (1992). A strong biological response to oceanic flow past Cobb Seamount. *Deep Sea Research Part A. Oceanographic Research Papers*, *39*(7-8), 1139-1145.

Duarte, C. M., & Cebrián, J. (1996). The fate of marine autotrophic production. *Limnology and Oceanography*, *41*(8), 1758-1766.

Dugdale, R. C. & Goering, J. J. (1967). Uptake of new and regenerated forms of nitrogen in primary productivity. *Limnology and Oceanography*, 12, 196-206.

Durães, M. F., de Mello, C. R., & Beskow, S. (2016). Trends in the hydrometeorological regime on an island in the South Atlantic Ocean. *Revista Brasileira de Climatologia*, *18*.

Evans, D. L., & Signorini, S. S. (1985). Vertical structure of the Brazil Current. *Nature*, *315*(6014), 48.

Evans, D. L., Signorini, S. R., & Miranda, L. B. (1983). A note on the transport of the Brazil Current. *Journal of Physical Oceanography*, *13*(9), 1732-1738.

Fanning, K. A. (1992). Nutrient provinces in the sea: concentration ratios, reaction rate ratios, and ideal covariation. *Journal of Geophysical Research: Oceans*, *97*(C4), 5693-5712.

Fernandes, A. M., da Silveira, I. C., Calado, L., Campos, E. J., & Paiva, A. M. (2009). A two-layer approximation to the Brazil Current–Intermediate Western Boundary Current System between 20° S and 28° S. *Ocean Modelling*, *29*(2), 154-158.

Furuya, K. (1990). Subsurface chlorophyll maximum in the tropical and subtropical western Pacific Ocean: Vertical profiles of phytoplankton biomass and its relationship with chlorophylla and particulate organic carbon. *Marine Biology*, *107*(3), 529-539.

Gaeta, S. A., Lorenzzetti, J. A., Miranda, L. D., Susini-Ribeiro, S. M., Pompeu, M., & Araujo, C. E. (1999). The Vitória Eddy and its relation to the phytoplankton biomass and primary productivity during the austral fall of 1995. *Archive of Fishery and Marine Research*, *47*(2/3), 253-270.

Garzoli, S. L., Dong, S., Fine, R., Meinen, C. S., Perez, R. C., Schmid, C., ... & Yao, Q. (2015). The fate of the deep western boundary current in the South Atlantic. *Deep Sea Research Part I: Oceanographic Research Papers*, *103*, 125-136.

Genin, A., & Boehlert, G. W. (1985). Dynamics of temperature and chlorophyll structures above a seamount: an oceanic experiment. *Journal of Marine Research*, *43*(4), 907-924.

Ghisolfi, R. D., da Silva, M. P., dos Santos, F. T., Servino, R. N., Cirano, M., & Thompson, F. L. (2015). Physical forcing mechanisms controlling the variability of chlorophyll-a over the Royal-Charlotte and Abrolhos Banks—eastern Brazilian shelf. *PloS one*, *10*(2), e0117082.

Gordon, A. L., Weiss, R. F., Smethie Jr, W. M., & Warner, M. J. (1992). Thermocline and intermediate water communication between the South Atlantic and Indian Oceans. *Journal of Geophysical Research: Oceans*, *97*(C5), 7223-7240.

Gove, J. M., McManus, M. A., Neuheimer, A. B., Polovina, J. J., Drazen, J. C., Smith, C. R., Merrifield, M. A., Friedlander, A. M., Ehses, J. S., Young, C. W., Dillon, A. K. & Williams, G. J. (2016). Near-island biological hotspots in barren ocean basins. *Nature Communications*, 7, 10581, doi: 10.1038/ncomms10581.

Graham, N. A. J., & Nash, K. L. (2013). The importance of structural complexity in coral reef ecosystems. *Coral Reefs*, *32*(2), 315-326.

Grasshoff, K., Kremling, K., & Ehrhardt, M. (1999). *Methods of seawater analysis*. John Wiley & Sons, Germany, 634 p.

Guglielmi, V., Goyet, C., Touratier, F., & El Jai, M. (2017). Generalized total least squares to characterize biogeochemical processes of the ocean. *Ocean Dynamics*, *67*(1), 37-49.

Hasegawa, D., Lewis, M. R., & Gangopadhyay, A. (2009). How islands cause phytoplankton to bloom in their wakes. *Geophysical Research Letters*, *36*(20).

Hasegawa, D., Yamazaki, H., Lueck, R. G., & Seuront, L. (2004). How islands stir and fertilize the upper ocean. *Geophysical research letters*, *31*(16).

Herrford, J., Brandt, P., & Zenk, W. (2017). Property changes of deep and bottom waters in the Western Tropical Atlantic. *Deep Sea Research Part I: Oceanographic Research Papers*, *124*, 103-125.

Heywood, K. J., Barton, E. D., & Simpson, J. H. (1990). The effects of flow disturbance by an oceanic island. *Journal of Marine Research*, *48*(1), 55-73.

Huisman, J., Thi, N. N. P., Karl, D. M., & Sommeijer, B. (2006). Reduced mixing generates oscillations and chaos in the oceanic deep chlorophyll maximum. *Nature*, *439*(7074), 322.

Karstensen, J., & Tomczak, M. (1997). Ventilation processes and water mass ages in the thermocline of the southeast Indian Ocean. *Geophysical Research Letters*, *24*(22), 2777-2780.

Kolb, G. S., Ekholm, J. & Hambäck, P. A. (2010). Effects of seabird nesting colonies on algae and aquatic invertebrates in coastal waters. *Mar Ecol Prog Ser*, 417, 287-300.

Lalli, C. M. & Parsons, T. R. (1997). *Biological Oceanography: an introduction*. Elsevier Butterworth-Heinemann, Oxford, 335 p.

Lavelle, J. W., & Mohn, C. (2010). Motion, commotion, and biophysical connections at deep ocean seamounts. *Oceanography*, *23*(1), 90-103.

Lee, K., Choi, S. D., Park, G. H., Wanninkhof, R., Peng, T. H., Key, R. M., ... & Kozyr, A. (2003). An updated anthropogenic CO2 inventory in the Atlantic Ocean. *Global Biogeochemical Cycles*, *17*(4).

Lemos, A. T., Ghisolfi, R. D. R., & Mazzini, P. L. F. (2018). Annual phytoplankton blooming using satellite-derived chlorophyll-a data around the Vitória-Trindade Chain, Southeastern Brazil. *Deep Sea Research Part I: Oceanographic Research Papers*, *136*, 62-71.

Levitus, S., Conkright, M. E., Reid, J. L., Nasjar, R. J. & Mantyla, A. (1993). Distribution of nitrate, phosphate and silicate in the world oceans. *Prog. Oceanog,* 31, 245-273.

Li, Y. H., Karl, D. M., Winn, C. D., Mackenzie, F. T., & Gans, K. (2000). Remineralization ratios in the subtropical North Pacific gyre. *Aquatic Geochemistry*, *6*(1), 65-85.

Libes, S. M. (2009). *Introduction to marine biogeochemistry*. Academic Press., Elsevier, United States of America, 925 p.

Liu, M., & Tanhua, T. (2019). Characteristics of Water Masses in the Atlantic Ocean based on GLODAPv2 data. *Ocean Sci. Discuss*., https://doi.org/10.5194/os-2018-139, in review.

Louanchi, F., & Najjar, R. G. (2000). A global monthly climatology of phosphate, nitrate, and silicate in the upper ocean: Spring-summer export production and shallow remineralization. *Global Biogeochemical Cycles*, *14*(3), 957-977.

Lueck, R. G., & Mudge, T. D. (1997). Topographically induced mixing around a shallow seamount. *Science*, *276*(5320), 1831-1833.

M.D.N.M. Braid. (2008). Caracterização da região oceânica da Cadeia Vitória-Trindade com base na avaliação dos parâmetros físico-químicos da coluna d' água. *Thesis*, 182 p.

Ma, J., Song, J., Li, X., Yuan, H., Li, N., Duan, L., & Wang, Q. (2019). Environmental characteristics in three seamount areas of the Tropical Western Pacific Ocean: Focusing on nutrients. *Marine Pollution Bulletin*, *143*, 163-174.

Mawji, E., Schlitzer, R., Dodas, E. M., Abadie, C., Abouchami, W., Anderson, R. F., ... & Bluhm, K. (2015). The GEOTRACES intermediate data product 2014.

McManus, M. A., Benoit-Bird, K. J., & Woodson, C. B. (2008). Behavior exceeds physical forcing in the diel horizontal migration of the midwater sound-scattering layer in Hawaiian waters. *Marine Ecology Progress Series*, *365*, 91-101.

Meirelles, P. M., Amado-Filho, G. M., Pereira-Filho, G. H., Pinheiro, H. T., De Moura, R. L., Joyeux, J. C., ... & Paranhos, R. (2015). Baseline assessment of mesophotic reefs of the Vitória-Trindade seamount chain based on water quality, microbial diversity, benthic cover and fish biomass data. *PloS one*, *10*(6), e0130084.

Mémery, L., Arhan, M., Álvarez-Salgado, X. A., Messias, M. J., Mercier, H., Castro, C. G., & Ríos, A. F. (2000). The water masses along the western boundary of the south and equatorial Atlantic. *Progress in Oceanography*, *47*(1), 69-98.

Mohr, L. V., Castro, J. W. A., Costa, P. M. S., & Alves, R. J. V. (2009). Ilhas oceânicas brasileiras: da pesquisa ao manejo. *MMA Secretaria de. Biodiversidade e Florestas*, Brasília, 2, 502 p.

Monterey, G., & Levitus, S. (1997). NOAA Atlas NESDIS 14. In *Seasonal variability of mixed layer depth for the world ocean*. Natl. Oceanic and Atmos. Admin. Silver Spring, Md.

Motoki, A., Motoki, K. F., & de Melo, D. P. (2012). Caracterização da morfologia submarina da Cadeia Vitória-Trindade e áreas adjacentes, ES, com base na batimetria predita do TOPO versão 14.1. *Revista Brasileira de Geomorfologia*, *13*(2).

Papiol, V., Cartes, J. E., Vélez-Belchí, P., & Martín-Sosa, P. (2019). Near-bottom zooplankton over three seamounts in the east Canary Islands: Influence of environmental variables on distribution and composition. *Deep Sea Research Part I: Oceanographic Research Papers*, doi: https://doi.org/10.1016/j.dsr.2019.04.003.

Pereira-Filho, G. H., Amado-Filho, G. M., de Moura, R. L., Bastos, A. C., Guimarães, S. M., Salgado, L. T., ... & Brasileiro, P. S. (2011). Extensive rhodolith beds cover the summits of southwestern Atlantic Ocean seamounts. *Journal of coastal research*, *28*(1), 261-269.

Perry, M. J., Sackmann, B. S., Eriksen, C. C., & Lee, C. M. (2008). Seaglider observations of blooms and subsurface chlorophyll maxima off the Washington coast. *Limnology and Oceanography*, *53*(5part2), 2169-2179.

Pianca, C., Mazzini, P. L. F., & Siegle, E. (2010). Brazilian offshore wave climate based on NWW3 reanalysis. *Brazilian Journal of Oceanography*, *58*(1), 53-70.

Pinheiro, H. T., Bernardi, G., Simon, T., Joyeux, J-C., Macieira, R. M., Gasparini, J. L., Rocha, C. & Rocha, L. A. (2017). Island biogeography of marine organisms. *Nature*, 549, 82-86.

Pinheiro, H. T., Mazzei, E., Moura, R. L., Amado-Filho, G. M., Carvalho-Filho, A., Braga, A. C., ... & Francini-Filho, R. B. (2015). Fish biodiversity of the Vitória-Trindade Seamount Chain, southwestern Atlantic: an updated database. *PloS one*, *10*(3), e0118180.

Piola, A. R., & Gordon, A. L. (1989). Intermediate waters in the southwest South Atlantic. *Deep Sea Research Part A. Oceanographic Research Papers*, *36*(1), 1-16.

Poole, R., & Tomczak, M. (1999). Optimum multiparameter analysis of the water mass structure in the Atlantic Ocean thermocline. *Deep Sea Research Part I: Oceanographic Research Papers*, *46*(11), 1895-1921.

Proudman, J. (1916). On the motion of solids in a liquid possessing vorticity. *Proceedings of the Royal Society of London. Series A, Containing Papers of a Mathematical and Physical Character*, *92*(642), 408-424.

Provost, C., Escoffier, C., Maamaatuaiahutapu, K., Kartavtseff, A., & Garçon, V. (1999). Subtropical mode waters in the South Atlantic Ocean. *Journal of Geophysical Research: Oceans*, *104*(C9), 21033-21049.

Read, J., & Pollard, R. (2017). An introduction to the physical oceanography of six seamounts in the southwest Indian Ocean. *Deep Sea Research Part II: Topical Studies in Oceanography*, *136*, 44-58.

Redfield, A. C. (1963). The influence of organisms on the composition of seawater. *The sea*, *2*, 26-77.

Reid, S. B., Hirota, J., Young, R. E., & Hallacher, L. E. (1991). Mesopelagic-boundary community in Hawaii: micronekton at the interface between neritic and oceanic ecosystems. *Marine Biology*, *109*(3), 427-440.

Reynolds, S. E., Mather, R. L., Wolff, G. A., Williams, R. G., Landolfi, A., Sanders, R. & Woodwards, M. S. (2007). How widespread and important is N2 fixation in the North Atlantic Ocean? *Global Biogeochemical Cycles*, 21, GB4015, doi:10.1029/2006GB002886.

Rezende, C. E., Andrade, L., Suzuki, M. S., Faro, B. C. M. T., Gonzalez, A. S. M., Paranhos, R., & Valentin, J. L. (2006). Caracterısticas hidrobiológicas da regiao central da Zona Econômica Exclusiva brasileira (Salvador, BA, ao Cabo de Sao Tomé, RJ). *REVIZEE/SCORE Central*.

Rezende, C. E., Andrade, L., Suzuki, M. S., Faro, B. C. M. T., Gonzalez, A. S. M., Paranhos, R., & Valentin, J. L. (2006). Caracterısticas hidrobiológicas da regiao central da Zona Econômica Exclusiva brasileira (Salvador, BA, ao Cabo de Sao Tomé, RJ). *REVIZEE/SCORE Central*.

Roesler, C., Uitz, J., Claustre, H., Boss, E., Xing, X., Organelli, E., ... & d'Ortenzio, F. (2017). Recommendations for obtaining unbiased chlorophyll estimates from in situ chlorophyll fluorometers: A global analysis of WET Labs ECO sensors. *Limnology and Oceanography: Methods*, *15*(6), 572-585.

Rogers, A. D. 2018. The biology of seamounts: 25 years on. *Advances in Marine Biology*, doi: https://doi.org/10.1016/bs.amb.2018.06.001.

Sato, O. T., & Polito, P. S. (2014). Observation of South Atlantic subtropical mode waters with Argo profiling float data. *Journal of Geophysical Research: Oceans*, *119*(5), 2860-2881.

Schlitzer, R., 2017. Ocean Data View, ⟨http://odv.awi.de⟩.

Schmid, C., Schäfer, H., Zenk, W., & Podestá, G. (1995). The Vitória eddy and its relation to the Brazil Current. *Journal of physical oceanography*, *25*(11), 2532-2546.

Shulenberger, E., & Reid, J. L. (1981). The Pacific shallow oxygen maximum, deep chlorophyll maximum, and primary productivity, reconsidered. *Deep Sea Research Part A. Oceanographic Research Papers*, *28*(9), 901-919.

Signorini, S. R., de Miranda, L. B., Evans, D. L., & Stevenson, M. R. (1989). Corrente do Brasil: estrutura térmica entre 19º e 25ºS e circulação geostrófica. *Boletim do Instituto Oceanográfico*, *37*(1), 33-49.

Skolotnev, S. G., Peyve, A. A., & Turko, N. N. (2010, April). New data on the structure of the Vitoria-Trindade seamount chain (western Brazil basin, South Atlantic). In *Doklady Earth Sciences* (Vol. 431, No. 2, pp. 435-440). SP MAIK Nauka/Interperiodica.

Sonnekus, M. J., Bornman, T. G., & Campbell, E. E. (2017). Phytoplankton and nutrient dynamics of six South West Indian Ocean seamounts. *Deep Sea Research Part II: Topical Studies in Oceanography*, *136*, 59-72.

Soutelino, R. G., Da Silveira, I. C. A., Gangopadhyay, A. A. M. J., & Miranda, J. A. (2011). Is the Brazil Current eddy-dominated to the north of 20 S?. *Geophysical Research Letters*, *38*(3).

Soutelino, R. G., Gangopadhyay, A., & Da Silveira, I. C. A. (2013). The roles of vertical shear and topography on the eddy formation near the site of origin of the Brazil Current. *Continental Shelf Research*, *70*, 46-60.

Sprintall, J., & Tomczak, M. (1993). On the formation of Central Water and thermocline ventilation in the southern hemisphere. *Deep Sea Research Part I: Oceanographic Research Papers*, *40*(4), 827-848.

Stramma, L., & England, M. (1999). On the water masses and mean circulation of the South Atlantic Ocean. *Journal of Geophysical Research: Oceans*, *104*(C9), 20863-20883.

Stramma, L., & Schott, F. (1999). The mean flow field of the tropical Atlantic Ocean. *Deep Sea Research Part II: Topical Studies in Oceanography*, *46*(1-2), 279-303.

Stramma, L.; lkeda, Y. & Peterson, R G. (1990). Geostrophic transport in the Brazil Current region. *Deep-Sea. Res*., 37(1A), 1875-1886.

Street, J. H., Knee, K. L., Grossman, E. E. & Paytan, A. (2008). Submarine groundwater discharge and nutrient addition to the coastal zone and coral reefs of leeward Hawaii. *Mar. Chem.*, 109, 355–376.

Takahashi, T., Broecker, W. S., & Langer, S. (1985). Redfield ratio based on chemical data from isopycnal surfaces. *Journal of Geophysical Research: Oceans*, *90*(C4), 6907-6924.

Talley, L. D. (1996). Antarctic Intermediate Water in the South Atlantic. In: *The South Atlantic: Present and Past Circulation*. Wefer, G.,Berger, W. H., Siedler, G., Webb, D. J. Springer-Verlag, Berlin Heidelberg, pp 219-238.

Taylor, G. I. (1917). Motion of solids in fluids when the flow is not irrotational. *Proceedings of the Royal Society of London. Series A, Containing Papers of a Mathematical and Physical Character*, *93*(648), 99-113.

Tomczak Jr, M. (1981). A multi-parameter extension of temperature/salinity diagram techniques for the analysis of non-isopycnal mixing. *Progress in Oceanography*, *10*(3), 147-171.

Tomczak, M., & Large, D. G. (1989). Optimum multiparameter analysis of mixing in the thermocline of the eastern Indian Ocean. *Journal of Geophysical Research: Oceans*, *94*(C11), 16141-16149.

Toole, J. M., Schmitt, R. W., Polzin, K. L. & Kunze, E. (1997). Near-boundary mixing above the flanks of a mid-latitude seamount. *Journal of Geophysical Research* 102, 947–959.

Tsuchiya, M., Talley, L. D., & McCartney, M. S. (1994). Water-mass distributions in the western South Atlantic; A section from South Georgia Island (54S) northward across the equator. *Journal of Marine Research*, *52*(1), 55-81.

Vanicek, M., & Siedler, G. (2002). Zonal fluxes in the deep water layers of the western South Atlantic Ocean. *Journal of Physical Oceanography*, *32*(8), 2205-2235.

Warner, M. J., & Weiss, R. F. (1992). Chlorofluoromethanes in South Atlantic Antartic intermediate water. *Deep Sea Research Part A. Oceanographic Research Papers*, *39*(11-12), 2053-2075.

White, M., Bashmachnikov, I., Arístegui, J. & Martins, A. (2007). Physical processes and seamount productivity. In: *Seamounts: Ecology, Fisheries & Conservation*. Pitcher, T.J., Morato, T., Hart, P.J.B., Clark, M.R.,Haggan, N., Santos, R.S. Fish and Aquatic Resources Series 12. Blackwell Publishing, Oxford, 65 -84.

Wyrtki, K. (1962, January). The oxygen minima in relation to ocean circulation. In *Deep Sea Research and Oceanographic Abstracts* (Vol. 9, No. 1-2, pp. 11-23). Elsevier.

Yesson, C., Clark, M. R., Taylor, M. L., & Rogers, A. D. (2011). The global distribution of seamounts based on 30 arc seconds bathymetry data. *Deep Sea Research Part I: Oceanographic Research Papers*, *58*(4), 442-453.